



# Hydraulic Properties Investigation of the Potters For Peace Colloidal Silver Impregnated, Ceramic Filter

Christopher J. Fahlin
Undergraduate Independent Study Research
University of Colorado at Boulder
College of Engineering
Advising Professor: Dr. Angela Bielefeldt
March 7, 2003

# Table of Contents

# Table of Figures

# Tables



# Acknowledgements

This research would not have been possible without the assistance of many people. I would like to thank Ron Rivera of Potters For Peace for his expertise, support, hospitality, and his quick and consistent communication. Without Ron's invitation, I would not have had the opportunity to travel to Nicaragua to start this investigation of the Potters For Peace filter. Thomas Davinroy, Director of the Undergraduate Research Opportunity Program (UROP), who made my trip to Nicaragua and subsequent research fiscally possible. I am extremely grateful for his flexibility and the time he spent working the details of the proposal at the last minute. I would also like to thank him for his quick turn-around on my proposal to leave for Nicaragua in less than 2 weeks, which proved to be crucial. Dr. Angela Bielefeldt, has motivated, guided, and encouraged me from the moment this project began in her class. I need to thank her for her patience, support, compassion, technical proficiency, and time. This research is truly one of the hardest challenges I have had to endure and without Angela's knowledge and support this research would not have made it to this finished state. Thank you, Angela. And most importantly, I would like to thank my wife. She always paid the rent, cooked my meals, and washed my clothes. Without her, I would be homeless, stinky, and starving. She encouraged me through the long and tedious hours of this research and I look forward to our new adventure with our baby due in July 2003[1].

[1] There were many other people directly involved with other aspects of my involvement with this filter and they are mentioned in the acknowledgements on the CD provided with this report.

# Abstract

This study investigated the hydraulic properties of the Potters For Peace filter in greater detail than previous studies by Sten Eriksen and Daniele Lantagne. Hydraulic properties such as the hydraulic conductivity and tortuosity are important because they help determine the contact time of pathogens in the water with silver to provide inactivation. Two laboratory tests were conducted using both experimental and numerical methods for attaining the results. Unfortunately, the hydraulic conductivity results were questionable for many reasons and the tortuosity results varied considerably due to the porosity variability results. This research does not conclusively describe the hydraulic properties for the PFP ceramic filter, but it does have model improvements and many recommendations for future research. Future work resulting from this research will hopefully lead to accurate and conclusive results about the hydraulic properties of this economically feasible and effective filter.

# Executive Summary

## INTRODUCTION

The Potters for Peace colloidal silver impregnated ceramic filter is an affordable sustainable technology for treating drinking water in individual homes of developing communities. Potters in many countries around the world produce this filter, the Filtrón. The most accomplished workshop is in Managua, Nicaragua.

The purpose of this research is to investigate the hydraulic properties of 5 filters from the Managua workshop. These properties are important because they help determine the contact time of pathogens in the water with silver to provide inactivation. Both experimental and numerical methods were used for the two laboratory tests that were conducted. The first test evaluated the hydraulic conductivity of each filter using various constant flow rates of deionized Boulder, Colorado, tap water. The second test used bromide as a tracer to calculate the tortuosity of pores in the ceramic. Results from this work led to recommendations for future study and improvements to silver application.

## BACKGROUND

Few studies have extensively evaluated the hydraulic properties of the Filtrón. In 2001, Sten Eriksen produced the first theoretical mathematical model to describe water flow through the filter. Daniele Lantagne conducted an extensive study of both the intrinsic effectiveness in the laboratory and a field study of the filter in Nicaragua, completed in December 2001. She also updated Eriksen's Model. The main technical theories utilized for the research are Darcy's Law and correlations to saturated groundwater contaminant transport.

Table ES-1 defines the parameters used and Figure ES-1 illustrates Le and Ls on the next page.

**Table ES-1: Parameter Defintions**

| Parameter | Units | Description |
|---|---|---|
| **Q** | mL/min | Flow through the filter; $Q = KA\frac{\Delta h}{L}$ |
| **K** | cm/min | Hydraulic conductivity (measure of how well water travels through the media) |
| **A** | $cm^2$ | Cross Sectional Area of the filter the water travels through |
| **?h** | cm | Difference in head between the influent and effluent of the filter |
| **L** | cm | Shortest linear length the water travels through the filter |
| **D** | $cm^2$/min | Dispersion coefficient (movement of molecules away from each other); $D = D_m t + a_L v$ |
| **$D_m$** | $cm^2$/min | Molecular dispersion coefficient of the tracer used (bromide) |
| **t** | unitless | Tortuosity is the ratio of the actual distance the water travels over the shortest linear length; $t = \frac{Le}{Ls}$ |
| **$a_L$** | cm | Longitudinal dispersivity, which is a property of the porous medium and is related to pore structure. |
| ***v*** | cm/min | Theoretical actual velocity of the water through the pores – should not be confused with Darcy's velocity |
| **Le** | cm | Theoretical actual distance the water travels |
| **Ls** | cm | Shortest linear length the water travels through the filter |

**Figure ES-1: Le and Ls Illustration**

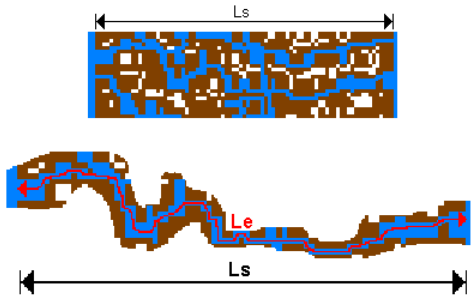


## Previous Studies and Model Comparison

Eriksen assumed the filter to be cylindrical while this research uses the true conical geometry of the filter. Figure ES-2 shows the cylindrical and conical shape used as well as the parameter definitions such as S, x, r, and so on.

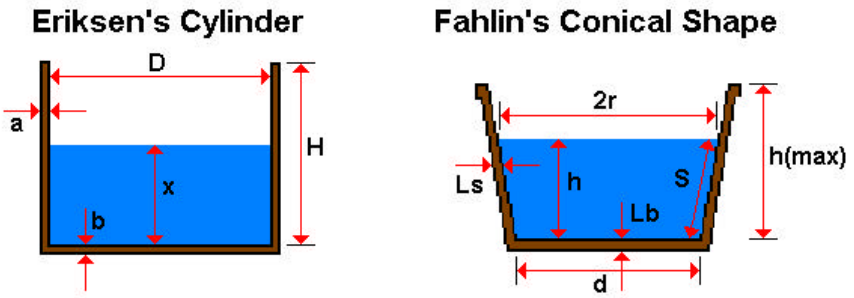


**Figure ES-2: Eriksen and Fahlin Geometric Models Comparison**

Eriksen assumed the filter was geometrically cylindrical using the average diameter between the top and bottom. Other key assumptions of both models are summarized in Table ES-2:

| Assumption Categories | Eriksen | Fahlin |
|---|---|---|
| **Geometry** | Cylindrical | Conical |
| **Hydraulic Conductivity** | Bottom and side conductivities are equal. | Bottom and side conductivities are different due to dissimilar compression forces during construction. |
| **Head** | Same head driving the flow through the bottom as the sides. | Head driving the flow through the bottom and sides is different. |
| **Overall water flow** | Batch process (completely filled with no water added). | Continuous flow (water pumped in at constant rates). |
| **Water flow the through sides** | Average flow through the sides by integrating Darcy's Law. | No integration since continuous flow was used. |

**Table ES-2: Assumption Comparison**

Eriksen derived two main equations to describe the flow of the filter for two reasons – (1) to find the actual hydraulic conductivity of the filter and (2) to calculate the theoretical maximum hydraulic conductivity. His model is used to describe the flow of water through the filter when it is initially filled completely, and then allowed to drain.

**Table ES-3: Eriksen Parameter Definitions**

| Parameter | Units | Origin | Description |
|---|---|---|---|
| $\mathbf{k_{actual}}$ | m/hr | Calculated | Actual hydraulic conductivity of the filter |
| $\mathbf{k_{max}}$ | m/hr | Calculated | Theoretical maximum hydraulic conductivity of the filter that should give sufficient silver contact time to inactivate pathogens. |
| **b** | m | Measured | Thickness of the filter bottom, which was assumed to equal the thickness on the side |
| $\mathbf{T_{min}}$ | min | Theoretical | Minimum time needed for silver inactivation |
| **T** | min | Measured | Time filter operated before x was measured |
| **c** | m | Assumed | Thickness of the colloidal silver layer |
| **H** | m | Measured | Height of the water inside the filter |
| **D** | m | Measured | Average diameter of the filter |
| **x** | m | Measured | Distance in height of the water at time of operation after it was filled completely to H. |

In Lantagne's work, the experimental pathogen inactivation achieved was significantly greater than predicted by Eriksen. Therefore, Daniele Lantagne reevaluated the Eriksen mathematical model in Section 5.1.2 of *Report 1: Intrinsic Effectiveness* (3). In that section, she explained his model and improved some of his values that he used with the model, but did not make any additions to the model except the tortuosity factor. She improved his time estimate for a filter to completely enter and the thickness of the colloidal silver layer (c) by using an assumed tortuosity. Table ES-4 is their results.

**Table ES-4: Previous Studies Hydraulic Conductivity Results**

| | Equation | Units | Eriksen | Lantagne |
|---|---|---|---|---|
| $\mathbf{k_{actual}}$ | $k_{actual} = \frac{b}{T}\ln\left[\frac{H}{x\left(1+\frac{2H}{D}\right)}\right]$ | m/hr | 0.03 | 0.004 |
| $\mathbf{k_{max}}$ | $k_{max} = \frac{cb}{T_{min}H}$ | m/hr | 0.00001 | 0.0004 |
| **ratio** | $\frac{k_{actual}}{k_{max}}$ | unitless | 3000 | 10 |

The results in Table ES-4 show that the actual conductivities were much larger than the actual conductivities leading to the conclusion that the filter has inadequate contact time with silver, but this differs from the empirical removal results of 98 to 100%. Ms. Lantagne's improvements were better estimates of the actual and maximum hydraulic conductivities; however there was still some question about why the filter is so effective and why the theory could not mathematically substantiate it.

## METHODS

Both experimental and numerical methods were used for this research. In the lab to ascertain the hydraulic conductivities, the area of filtration was kept constant by using constant flow to simplify the determination of hydraulic conductivities. Also in the lab, bromide was used as a tracer for the first attempt to measure the tortuosity of the filter by recording its breakthrough times. For the numerical methods, graphical analysis and Excel® Solver were used.

## DISCUSSION OF RESULTS

The results of this research are not definitive; they are only a beginning for future research. While conducting the hydraulic conductivities test, the filters experienced a clogging phenomenon that hindered the results. The conductivity results were also hindered due to the inadequate side head modeling with Darcy's Law. At best, the hydraulic conductivity results have two results that seem to be logical for two filters. Overall, the hydraulic conductivity results are not similar in magnitude or trends, thus they are inconclusive.

The bromide tracer breakthrough tests are more useful and could be refined with accurate volumetric porosity measurements of the filters used in this research. According to the results, the water remains in the filter for a considerable amount of time. The earliest the bromide tracer could be detected in the initial breakthrough time was 50 minutes at the high flow rate. It is the minimum amount of time the tracer could be detected coming out of the receptacle, not the contact time with silver. The 50 minutes initial breakthrough result is likely to be a good estimate of the minimum amount of time the water is in the pores of the filter.

Assuming this estimation is correct, there should be plenty of time for contact with the silver depending on the thickness of the silver layer. If the silver completely lined the internal pore surface of the filter from the inside to the outside, 50 minutes at a lower concentration of silver

currently used by Potters for Peace should be adequate for inactivation. This is assuming that the 25 minute minimum contact time used by Eriksen and the 20 minute contact time from Microdyn (the manufacturer of the colloidal silver) has any merit with regard to a desirable inactivation (such as 99.9%).

The tortuosity results ranged from 4 to 19, but if the overall porosity of the filters were known through experimental analysis these numbers could be refined and quickly determined by using the same spreadsheets constructed for this research. Since the porosities were determined by numerical methods, an estimation of the colloidal silver layer was also determined for each filter. The colloidal silver layer ranged from 2.5 to 10 mm.

Table ES-5 summarizes all of the Fahlin's results assuming the initial Eriksen Model is valid by comparing the values with Eriksen's initial guess and Lantagne's corrected update.

| Parameter | Units | Eriksen | Lantagne | Fahlin | |
|---|---|---|---|---|---|
| $k_{actual}$ | m/hr | 0.03 | 0.004 | 0.00104 | 0.00287 |
| $k_{max} = \frac{ctb}{T_{min} H}$ | | | | | |
| ***c*** | m | 0.0001 | 0.0020 | 0.0025 | 0.0100 |
| **t** | - | 1 | 2 | 4 | 19 |
| ***b*** | m | 0.010 | 0.010 | 0.0145 | 0.0145 |
| $T_{min}$ | min | 25 | 25 | 25 | 25 |
| ***H*** | m | 0.24 | 0.24 | 0.2034 | 0.2034 |
| $k_{max}$ | m/hr | 0.00001 | 0.00040 | 0.00171 | 0.00325 |
| $\frac{k_{actual}}{k_{max}}$ | - | 3000 | 10 | 0.61 | 0.89 |

**Table ES-5: Overall Result Summary Compared to Previous Studies**

## RECOMMENDATIONS

Unfortunately for Potters For Peace, there is only one immediate recommendation; however, there are recommendations for future research. Hopefully, results from future research will clear-up many uncertainties contained in this research and give Potters For Peace something tangible and more useful in the future.

Both the clogging phenomena and the porosity results indicate that entire pore structure is not fully utilized with a colloidal silver layer. The only recommendation for Potters For Peace is to try new methods of colloidal silver application to fully utilize the entire path of water flow through the filter for contact with inactivating silver. The intended outcome from optimizing the colloidal silver application could be extending the time of use, or life, of the filter by reducing the internal biological clogging while maintaining a high removal percentage and keeping the cost either the same or lower.

There are six future research recommendations. The first three are directly related to this research and last three are not:

1. Repeat the hydraulic conductivity test with slightly different methods ensuring no the filters are covered from light exposure, improved water quality is used, and using all data collected so as not to assume a linear relationship between flow rate and area.

2. Model the side head so Darcy's Law could be used more accurately.

3. Directly measuring the overall volumetric porosity of each filter used in this research so already collected data could be fully utilized to accurately solve for the tortuosity and colloidal silver layer thickness.

4. Determine the Contact Time (CT) for Microdyn's colloidal silver inactivation of pathogens to optimally use the colloidal silver resource i.e. less or more silver with enhanced performance (better inactivation with less clogging).

5. Silver stripping research to determine a silver effluent concentration that could be supported and connected by the CT research.

6. Electron Microscope research of the bottom and side pores structure of the filters used in this research since only a lip of a filter has previously been analyzed.

## CONCLUSION

This research is a building block for future research and analysis of the hydraulic properties of the Potters For Peace colloid silver impregnated, ceramic filter. The initial goals were to find the hydraulic conductivities and tortuosity of the five filters tested. Unfortunately, the hydraulic conductivity results were questionable for many reasons and the tortuosity results varied considerably due to the porosity variability. However, there are some important conclusions found in this study as described below:

- Hydraulics of the filter are complex. This research developed an improved model of the actual conical shape of the filter so it is more applicable to the specifics of the constructed filters.
- Some clogging phenomenon occurred over time in the lab, which is also likely to occur in user homes. This is likely attributed to partial utilization of colloidal silver in the pore structure leaving room for biological growth on the non-lined surface of the pores.
- Further testing of colloidal silver inactivation and hydraulics is needed.

This research may not conclusively describe the hydraulic properties for the PFP ceramic filter, but it does have model improvements and many recommendations for future research. Future work resulting from this research will hopefully lead to accurate and conclusive results about the hydraulic properties of this economically feasible and effective filter.

(This page is intentionally left blank)

**Section 1.0 Introduction**

The Potters for Peace colloidal silver impregnated ceramic filter is an affordable sustainable technology for treating drinking water in individual homes of developing communities. Potters in many countries around the world including Mexico, Bangladesh, Cambodia, Haiti, Guatemala, El Salvador, Nepal, and Nicaragua produce this filter, the Filtrón. The most accomplished workshop is in Managua, Nicaragua. Four filters from the workshop were selected at random from the finished filters. Three are impregnated/lined with colloidal silver and one is not. An additional silver-lined filter was shipped from the workshop to me, Christopher Fahlin, during the summer of 2002. All five filters were used in this research.

The purpose of this research is to investigate the hydraulic properties, such as tortuosity and hydraulic conductivities, of the five Filtróns. These properties are important because they will help determine the contact time of pathogens in the water with silver to provide inactivation. Two tests were conducted. The first test evaluated the hydraulic conductivity of each filter using various constant flow rates of deionized Boulder, Colorado, tap water. Tests were conducted over a range of selected flow rates. The second test used Bromide as a tracer to calculate the tortuosity of pores in the ceramic. Hydraulic conductivity and toruosity properties are important not only because they will help determine the contact time for inactivation of pathogens by the silver, but because they will potentially lead to improvements in colloidal silver application.

There were two methods used to investigate the Filtrón – (1) experimental and (2) numerical. Following the methods section, the results will be presented and then discussed. Recommendations for future research and improvements for Filtrón quality control will follow the discussion. Ending this report are the conclusions. References used in this work are listed at the end of this report and can provide further information. Appendices contain details on specific experimental methods, derivations, and calculations.

## Section 2.0 Background

### 2.1 Motivation

As part of my undergraduate Bachelor of Science degree program in Environmental Engineering, I enrolled in the required course *CVEN 4434: Environmental Engineering Design* taught by Dr. Angela Bielefeldt during the fall 2001 semester. I was expecting to design local wastewater treatment plants because that had been the focus of the class in the past. To my surprise, the wastewater plant was only one of the three possible projects to choose. The other two projects were appropriate technology projects in developing communities identified by the University of Colorado's Engineers Without Borders (EWB) during the spring and summer 2001. Both projects had the potential to be implemented based on the student designs. I chose the San Pablo Water Management Project.

San Pablo is located on the Swasey River in the Toledo District of Belize, Central America. Originally, our project was to conduct an alternatives assessment of technologies and preliminary design for all of the water affecting the village of 250 people including wastewater, irrigation water, and drinking water. This proved to be much too large of a project for a team of three undergraduates in a single semester so we decided to focus only on drinking water treatment. We decided on drinking water treatment because we felt it was the highest priority to improve the health of the villagers. Once the water is treated, the people would be less sick and more time could be spent working or in school. Our decision to focus on the drinking water occurred around the end of September 2001.

I decided to visit Water for People (WFP) in Denver in early October since we had never done a project like this or been formally taught how to approach this type of project. WFP is a non-profit organization that is associated with the American Waterworks Association (AWWA) and they have extensive experience with our type of project. I met with Jody Camp, Projects Manager, during the fall break for about three hours. During our meeting, she informed me about how they approach projects and what kind of projects they have done. At the end of our meeting, she gave me stacks of reference material that described past projects and lessons learned.

**Figure 3: PFP Ceramic Filter (2)**

One of the project summaries she gave me was entitled the *Tarahumara Filter Project* (1) led by Potters for Peace (PFP), a United States-based non-governmental organization (NGO). The filter described in the project was a low-cost, artisan-made, colloidal silver impregnated ceramic water filter intended for use in households as point-of-use drinking-water treatment (See Figure 1).

The purpose of the filter is to remove pathogenic (disease causing) organisms from drinking water including bacteria, viruses, and protozoans. Potters for Peace introduces the filters "in developing countries first by establishing micro-enterprises of artisans making the filters, and then by partnering with NGOs that distribute the filters to families" (2). In Managua, Nicaragua, PFP works with a cooperative of potters to manufacture and market these filters (2).

The filters constructed in Managua are made with a sawdust and clay mixture that is first formed by a press then fired, cooled, tested, dried, and then the bacteriostatic colloidal silver is applied to the surface making the filter ready for sale. The mixture is comprised of a 40 sawdust to 60 clay volumetric ratio, and is mixed in a cement mixer with water for at least 10 minutes. After it is mixed, a cantaloupe sized ball of the mixture is put into the female part of the mold. Once in the mold, a 10-ton truck jack is used to press the male and female parts together to form the filter. This press method ensures better filter uniformity than hand forming. The next step is to fire a batch of 40 to 50 filters in a flattop kiln eventually reaching 887 $^{o}$C over an 8 to 9 hour period. This totally combusts all of the sawdust in the filter and makes it porous so that water can travel through the filter. The filter is allowed to cool before each filter is tested.

Each filter is tested by measuring the flow rate and making sure it is between one and two liters per hour. Any filter outside of the flow range is discarded and cannot be recycled (the clay is no longer usable for the filters since it was mixed with sawdust). Ron Rivera, the leading expert in the construction of the filter, determined the one to two liter flow range to ensure there is enough contact time between the silver and pathogens in the water to inactive them. A slower flow rate could provide sufficient inactivation but would be inconvenient for users.

After passing the flow test, the filters are allowed to dry before the colloidal silver is applied. The colloidal silver acts a bacteriostatic treatment via three mechanisms – (1) inhibiting functional enzymes in microorganisms, (2) interaction with cell walls, and (3) interaction with nucleic acids such as DNA (deoxyribonucleic acid) (3). The colloidal silver is applied by adding 2 mL of the industrial strength (3.2% by mass/volume) Microdyn silver solution to 250 mL of filtered water. The particle diameter of the colloids range from 1 to 1000 nanometers ($10^{-9}$ to $10^{-6}$ m) (4). The entire 252 mL solution is painted on the inner and outer filter surface with a paintbrush until the filter has adsorbed all of the solution.

According to the World Health Organization (WHO) drinking water needs are 2.5 liters per day per person. Therefore, one Filtrón for US$8 in Nicaragua is sufficient to treat enough drinking water for a family of nine for a year assuming the filter operates for 16 hours a day with a constant flow rate of 1.4 liters per hour. Included in the purchase would be an ethnographic operation and maintenance sticker, the filter, a five-gallon plastic receptacle with plastic spigot, and a lid. The receptacle can also be made of ceramic, but this costs a couple of extra dollars.

As previously mentioned, the colloidal silver inactivates pathogens; however, the silver is not the only form of pathogen removal. In fact, most of the pathogen removal is attributed to the small pore size of the filter. Potters for Peace aims to have a pore size of 1 micron to remove most of the disease causing agents larger than that size. A scanning electron microscope (SEM) analysis of the filter lip by Industrial Analytical Service, Inc. conducted during the fall of 2001 measured a pore size range of 0.6 to 3 microns (3). "The variation in pore size is due to the location of the

sawdust during firing" (3). The lip of the filter is the least compressed region of the filter so it is safe to assume they are within reasonable range of their 1 micron goal. Viruses are too small to be removed ranging "from 18 nm [0.018 microns] to several hundred nanometers (5)", but most bacteria and protozoa are larger than 1 micron including *Escherichia coli (E. coli)*, *Giardia*, and *Crytosporidium* (5).

There are two types of filter maintenance that are currently recommended by Potters for Peace – routine and yearly. On a routine basis, the filters should be scrubbed by some type of brush to remove the trapped particles on the surface. These particles include trapped microorganisms such as bacteria and protozoa and sediment in the raw water being treated. Also, the receptacle should be cleaned ideally with chlorine, if it is available, to ensure a more sterile environment to minimize bacteria growth in the receptacle after filtration causing water contamination. On a yearly basis, Potters for Peace recommends heating the filter in an oven at a baking temperature (which I assumed to be about 350$^{o}$F) or higher for at least 20 minutes and then relining the filter with colloidal silver. Potters For Peace did not state the exact temperature. The reheating would kill and destroy all pathogens trapped within the filter in addition to those on the surface.

From the discovery of the filter from Water For People, I researched as much as I could, which was mainly the Potters for Peace website – www.potpaz.org. The Nicaragua workshop is the most accomplished workshop at this time that produces the filters, which they call the Filtrón. I soon discovered that no comprehensive studies of the filter from the United States at that time (October 2001) had been completed. The only microbiological study that had been completed was done by the University of Nicaragua in Managua (7). I emailed Ron Rivera, the in-country supervisor for the Nicaragua workshop and champion of the filter, to get more information on the filter in the form of videotape. From that email, we started to correspond about my project and his projects and he invited me to stay in Managua, Nicaragua, to witness the construction and interview users of the Filtrón. Because there was little formal engineering information or literature on the filter, I was invited to Nicaragua to do some preliminary research. Therefore, I wrote an Undergraduate Research Opportunity Program (UROP) proposal to do lab work at the University of Colorado (CU) at Boulder and a brief field study in Nicaragua.

### 2.2 Original Research Goals

The original goals of the Undergraduate Research Opportunity Program (UROP) proposal were to conduct a brief user study in Nicaragua and a microbiological study in the labs at CU after returning from Nicaragua. UROP granted me the money, which paid for an interpreter, Alexandra Gabrieloff, and me to travel to Nicaragua as well as a few hundred dollars for lab costs once we returned. Two days before traveling to Nicaragua over the Thanksgiving break, Ron Rivera informed me of a study that was conducted during the late summer through October of 2001 by Alethia Environmental. Alethia, located in Allston, Massachusetts, is a sole proprietorship consulting firm specializing in water quality analysis and point-of-use water supply. Daniele Lantagne is the founder and sole proprietor. She is also a Massachusetts Institute of Technology (MIT) lecturer. Ms. Lantagne's reports were completed in December 2001 and covered all of the areas that I had originally wanted to research for UROP in great detail; however, she had many recommendations for future research. With those recommendations, I developed new research goals.

**2.3 Alethia Environmental Study**

The Alethia Environmental Study entitled *"Investigations of the Potters for Peace Colloidal Silver Impregnated Ceramic Filter"* is divided into two reports – *Report 1: Intrinsic Effectiveness* and *Report 2: Field Investigations*. The study was jointly funded by the United States Agency for International Development (USAID) and Jubliee House Community (JHC), an international Christian community that is a 501(c)3 organization in North Carolina (3). The study is extensive, covering a large spectrum of research topics ranging from the history of the filter and colloidal silver as a disinfectant, to microbiological removal by the Filtrón, and common problems experienced by users in the field. Specifically, the reports addressed each of the following:

Report 1: Intrinsic Effectiveness of the Potters for Peace Ceramic Filter

- Best practices for colloidal silver application.
- Expected filter flow rates with and without colloidal silver.
- Expected lifetime per application of colloidal silver.
- Concentration of silver in filtered water.
- Effects of ingestion of the silver.
- Inactivation of microbes as a function of the concentration of silver.
- Effectiveness of silver in removing other pollutants commonly found in the area of interest.

Report 2: Field Testing of the Potters for Peace Ceramic Filter

- Discussion of the performance of the filters under field conditions.
- Comparison of filter performance with other commonly used methods of treatment.

Ms. Lantagne sent me a rough draft of the reports before I went to Nicaragua and I soon realized that my initial research ideas in the proposal to UROP would no longer be helpful or possible. Lantagnes's study finally concluded that:

> This study agrees with historical data that shows that the PFP colloidal silver-impregnated ceramic filter design produces a filter capable of removing 100 percent of bacteria and bacterial indicators of disease-causing organisms. Although the ceramic filter itself removes a majority of the indicators, the colloidal silver is necessary to achieve 100-percent removal. However, research in homes using this filter indicates that this effectiveness is not matched in the field. An educational component that includes safe storage, aseptic cleaning procedures, and follow-up visits to ensure continued usage and replacement of broken pieces is necessary to ensure that the intrinsic effectiveness of this filter is matched in the field. Further research on the removal rates of protozoa, viruses, and contaminants, as well as the resistance of the colloidal silver layer to scrubbing, is needed. Based on these results it is concluded that… the PFP filter is an effective and appropriate technology that improves both water quality and human health. (2)

I did not have the time, the money, or the personnel to do a worthy comparable study focused on pathogen removal. I then decided to focus on her recommendations for future research.

She has many recommendations in her reports and I chose to focus on Section 5: Filtration Investigations of Report 1. Within this section, she reviewed the mechanisms of water flow through the filter, flow rate change over time, and analyzed filters with different flow rates for both colloidal silver concentration in the finished water and microbiological inactivation. As part of her review of the mechanisms of flow through the filter on page 36 of Report 1, she states, "…the tortuosity factor of the ceramic filter is estimated at a factor of 2. This also is an

estimate, and further analysis is also need to refine this factor." This factor was essential to predicting inactivation of pathogens by the Filtrón. The intent of my lab research is to further analyze the tortuosity factor by using saturated groundwater transport theory. Before I was able to do lab work, I had to retrieve the filters from Nicaragua.

### 2.4 Field Trip to Nicaragua

During Thanksgiving break 2001, Alexandra Gabrieloff and I traveled to Managua, Nicaragua for six days (2 days of travel and 4 days in country). Alexandra is originally from Colombia and she is the person who briefed our *CVEN 4484* design class on San Pablo and their engineering needs. She served as the Spanish interpreter for this project. We brought water sampling equipment, cameras, video cameras, and a portable turbidity meter. The water sampling equipment, which was held in Miami's United States (US) Customs for three days with the portable turbidity meter, was used to take samples on the last day from a small municipality called San Francisco Libré.

San Francisco Libré is located northeast and on the other side of Lago de Managua (Managua Lake) from Managua, the capital of Nicaragua (See Figure 2). It took about three to four hours to reach San Francisco Libré by truck from Managua. If Nicaragua had an adequate road system, the trip would have taken about a quarter of the time.


**Figure 4: Map of Nicaragua, Central America**

When we arrived in San Francisco Libré, we met with a non-governmental organization (NGO) called Alianza Medica Cristiana. They are the NGO that purchased the filters for the community. After we obtained their permission, they took us to a part of the community that had been using the filters for six months. We conducted verbal interviews of five households, took pictures, and sampled the water to be tested at Boulder County's Wastewater Treatment Plant for

pathogenic indicator bacteria. Before we traveled to San Francisco Libré, we were not able to visit other communities because our equipment was in Miami's US Customs; however, we were able to focus on the production of the filters and daily activities of the ceramic workshop in Nicaragua.

The Nicaraguan Filtrón workshop is located in Ciudad Sandino on the outskirts of Managua. During our visits to the workshop, we conducted interviews with the filter manager, Juan Carlos, and some of the potters. We also videotape recorded parts of the construction process and equipment. Ron Rivera has already made a comprehensive video of the construction. In addition, I picked four random filters that had passed the flow rate test (see next paragraph). Three filters had colloidal silver applied while the fourth filter did not. I subsequently used the filters in the laboratory for my research at CU. An additional used filter was brought back to Colorado from San Fransico Libré and it was my intention to test it; however, the founder of Engineers without Borders, Dr. Bernard Amadei, used it on his trip to Africa as a promotional and demonstrational tool. One more filter with colloidal silver was purchased from Potters for Peace to replace it during the summer of 2002 to make the total number of filters equal to five.

To ensure that the filters are working correctly, every filter's flow rate is tested at the workshop. Ron Rivera established a guideline of one to two liters per hour for the test. As long as the filter is within that range, it passes the test, colloidal silver is added, and then can be sold. Any filter outside the range is discarded. If the flow rate is too slow, the pore size is too small and will operate slowly with a higher chance to clog sooner and more frequently; therefore it is rejected based off user considerations for flow rate. Ron Rivera determined this guideline from the Mexico based colloidal silver manufacturer – Microdyn. The directions for drinking water disinfection are to add one drop of the 0.32 percent solution to two liters of water and wait 20 minutes (0.16 mg colloidal silver/L or 0.16 ppm colloidal silver). From the directions, Ron determined that for two liters of water to be safe to drink at least 20 minutes of contact with the silver is needed. Ron estimated with a safety factor of three that 60 minutes for two liters was sufficient for the water to be safe to drink. The safety factor was included since the water is not remaining still in the filter (3). Therefore, if the water passes through the Filtrón too quickly it is likely that is has had inadequate time to inactivate pathogens and is rejected. It must be noted that liquid concentrations of silver suspended in water required for pathogen inactivation are also not directly comparable to water contacting ceramic sorbed with silver.

After the trip to Nicaragua and reading Daniele Lantagne's investigation, I was able to confidently recommend the Filtrón for drinking water treatment in the village of San Pablo, Belize. Once our alternative assessment and preliminary design for the class was completed in December 2001, we sent it to Dr. Filiberto Peñados of the Maya Institute who had contact with San Pablo.

Dr. Peñados was extremely excited about the project so we pursued funding from Sustainable Village located in Boulder to conduct a feasibility study for our recommendation in San Pablo. Sustainable Village is an organization that specializes in connecting funders with under funded projects; however, this time it was Sustainable Village that funded us. The funding covered travel for three people (Hector Valdez, Ron Rivera, and I) and room and board for the trip. Engineers without Borders provided additional $400 for over budget expenses. (For more

information on the trip to Belize during Spring Break 2002, see the Filtrón Package CD) Once the Belize Filtrón Feasibility Report was finished in May 2002, I was finally able to start my laboratory research with the five filters.

### 2.5 Final Research Goals

My UROP proposal included my original research goals, which were to conduct a brief user study in Nicaragua and a microbiological study in the lab after returning from Nicaragua. As mentioned earlier, the final intent of my laboratory research is to further analyze the tortuosity factor and hydraulic conductivity of the filters. From the user study that I attempted in Nicaragua, only the results from the microbiological tests are useful. The interviews were inconclusive for many reasons, as will be discussed in Section 4.1 Field Results. As a result of the insufficient user study, the primary goal of my research is to further analyze the tortuosity factor and hydraulic conductivity of the Filtrón units using experimental and numerical methods.

### 2.6 Laboratory work

The laboratory work started in September and continued until early December 2002. There were two phases of the lab work – (1) Hydraulic Conductivity Tests and (2) Bromide Tracer Breakthrough Tests. Phase One was conducted from late September until Thanksgiving at the end of November 2002. During this phase, the surface area and the height of water within the filter were measured while varying the incoming flow rate. The goal was to have a constant flow rate (Q) to the filter produce a constant volume of water in the Filtrón, resulting in a constant surface area of filtration such that the hydraulic conductivity (K) could be easily calculated using Darcy's Law given the constant Q, surface area, and hydraulic gradient. Phase Two continued from the end of November until about the 10$^{th}$ of December. This phase measured the breakthrough in bromide concentration when it was introduced into the filter. Bromide was selected as non-reactive tracer chemical that would follow the water flow and be easy to measure. Bromide should not significantly sorb to the ceramic filter. In this way, bromide serves as a surrogate chemical to indicate how pathogens less than the filter pore size would move through the Filtrón. The electrical conductivity of the water coming out of filter was measured in Micro-Siemens (µS). Micro-Siemens are proportional to the concentration of the bromide ion ($Br^-$) in solution, so as the micro-Siemens increases so does the concentration of bromide. Phase Two was much shorter experimentally but involves more complex numerical methods to analyze the meaning of the results. The results yield more information than the basic constant head tests. More detail about the lab work will be given in Section 3.0 Methods.

### 2.7 History of the Filters Used

The history of the filters used is important to note since three of the five were used in some prior research. Filters 1, 3, and 4 were used for a nitrate study (6) completed by David DiGiacomo, Emily Heller, Leslie Martien, and Sarah Williams during the spring 2001 semester. They are undergraduates that completed the research as an independent research project for their *CVEN 3454: Water Quality* class taught by Professor Joseph Ryan at the University of Colorado at Boulder.

The potential impact of this information is that the filters may experience clogging sooner than if they had never been used before this research. They tested the filters over a three-week period using nitrate (10 to 20 mg nitrate/L) and particle rich water (turbidity 5 to 95 NTU) in some

cases. Total filtered water quantity was only 40 to 100 liters so minimal loss of silver likely occurred.

Filter 5 does not have colloidal silver applied and was not used for their study. Filters 1, 3, 4, and 5 are the filters I picked at the Nicaragua workshop during my trip. Filter 2 was an additional filter purchased during the summer of 2002 from Potters for Peace to replace the filter borrowed by Dr. Amadei. Filter 2 was also made in the Nicaragua workshop and is colloidal silver impregnated.

Before each of the filters were tested in this research, each filter was tested to confirm that the filtration rate remained in the acceptable 1 to 2 liter per hour flow rate range; the same test that is performed in Nicaragua during the production. All of the filters passed the test. Regrettably, the exact flow rates were not recorded. It was not my intention to test the loading of the filters for this research and that is why they were not recorded. However, it should be noted that Filter 4 had the slowest flow rate of all the filters and it barely passed the test. This observation corresponds to the one slow filter in the nitrate study (6).

### 2.8 Basic Filtrón Geometric Model

The geometric model used for the Filtrón in this research is a partial cone. Below are the schematics of the filter's geometry (not to scale) and its labels of parameters such as S, x, y, r, d, and h:

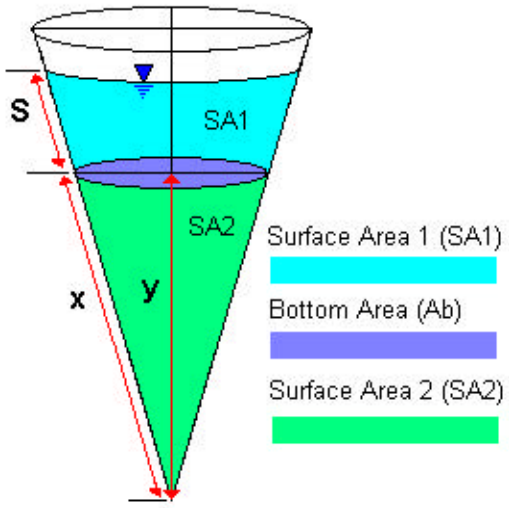


**Figure 5: Overall Inside Conical Geometry of the Filtrón**

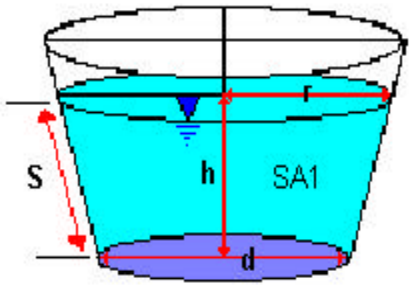


**Figure 6: Focused Internal Geometric Region of the Filtrón**

| Parameter | Definition |
|---|---|
| **S** | Length of side in the filter (internal side) from the bottom of the filter to the top of the water |
| **x** | Imaginary length of the side from the tip of the cone to the internal bottom of the filter |
| **y** | Imaginary height from the tip of the cone to internal bottom of the filter |
| **r** | Radius of the top of the water within the filter |
| **d** | Diameter of the internal bottom of the filter |
| **h** | Height of the water inside the filter |
| **Ab or $A_b$** | Actual surface area of the internal bottom of the filter |
| **SA1 or $SA_1$** | Actual side surface area of the filter |
| **SA2 or $SA_2$** | Imaginary side surface area of the bottom of the cone |
| **$SA_T$** | Total side surface area of the cone = $SA_1 + SA_2$ |
| **V1 or $V_1$** | Actual volume of water within the filter |
| **V2 or $V_2$** | Imaginary volume of the bottom of the cone |
| **$V_T$** | Total volume of the cone = $V_1 + V_2$ |

**Table 6: Geometric Parameters Defined**

Figure 3 illustrates the internal cone of the filter. The Filtrón has two cones that represent the complete geometric shape of the filter – one on the inside (or internal cone) and one on the outside. Only the cone on the inside will be used because Darcy's Law requires the surface area that the water travels through in the filter. Figure 4 is the actual internal geometric shape of the Filtrón. In other words, it is the shape of the water inside the filter. The real Filtrón has a lip on the upper circle to be used as the support in the receptacle; it is not included in this geometric model of the filter.

Each of the filters used in the experiments was measured separately for the parameters *S, h (max), d,* and the thicknesses of the bottom and sides – $L_b$ and $L_s$, respectively. The parameter *h (max)* is the maximum height of water within the filter once it is full. Similarly, *r (max)* is the radius of the water once the filter is full. The parameter *r (max)* is the maximum radius of the water within the filter and was calculated once *S* and *h (max)* were measured and the parameters *x* and *y* were calculated using similar triangles. On the next page are the equations and similar right triangle diagram used for the calculations (not to scale):

**Figure 7: Triangle Cross Section of the Internal Filtrón Cone**

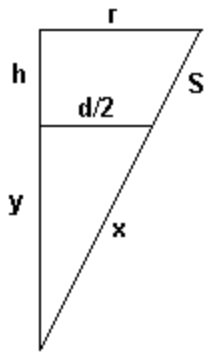


Figure 5 is used for the similar right triangles method for solving for *x* and *y*. First, I solved for *x* and then *y* using *x*:

$$\frac{r}{d/2} = \frac{S+x}{x} \Rightarrow x = \frac{Sd}{2(r - d/2)} \qquad (1)$$

Using Pythagoras' Theorem,

$$x^2 = (d/2)^2 + y^2 \Rightarrow y = \sqrt{(x^2 - (d/2)^2)} \qquad (2)$$

Once I calculated *x* and *y*, I then could calculate *r* using similar right triangles:

$$\frac{r}{d/2} = \frac{(h+y)}{y} \Rightarrow r = d/2 \frac{(h+y)}{y} \qquad (3)$$

With all the known parameters, the surface area can be calculated. The total surface area was calculated first:

$$SA_T = pr(S+x) = SA_1 + SA_2 \qquad (4)$$

$$SA_2 = px\,d/2 \qquad (5)$$

$$SA_1 = SA_T - SA_2 = \frac{pd}{2y}(hS + hx + yS) \qquad (6)$$

After *S, h (max),* and *d,* were measured, the parameters *x* and *y* were calculated and they remained constant for each filter. The only parameters that changed during the experiments were the actual *S, h, r, and SA1*. Thus, *SA2, x, y, d,* and $A_b$ remain constant for each filter. To check the validity of the model, I calculated the maximum volumes of each filter and checked against the measured volumes of four of the filters. The numerical results are in section 4.2 Basic Filtrón Characteristics. The overall conclusion is that this geometric model is reasonable and can be used. In fact, it is much better than the cylindrical assumptions in Eriksen's model, which will be discussed in the theory section. Below are the equations used for calculating the volumes:

First calculated the total volume:

$$V_T = \tfrac{1}{3}\pi r^2 (h + y) = V_2 + V_1 \quad (7)$$

$$V_2 = \tfrac{1}{3}\pi \frac{d^2}{4} y \quad (8)$$

$$V_1 = V_T - V_2 = \frac{\pi d^2}{12}\left[\frac{h^3 + 3hy^2 + 3h^2 y}{y^2}\right] \quad (9)$$

**2.9 Technical Theory**

This section is the most important section for understanding this report and my research. First, my interpretation of the text book descriptions and definitions of the basic water engineering principles used in this research will be discussed such as Darcy's Law, hydraulic conductivity, and tortuosity. Following the engineering principles, previous studies and their findings are described. Finally, ending this section will be a comparison between the previous studies and my research.

**2.9.1 Darcy's Law**

Darcy's Law is a fluid mechanics principal which represents the water velocity as it travels through porous media. It is the basic equation used in groundwater hydraulics (8). Equation 10 is the common form of Darcy's Equation that describes the relation between hydraulic gradient and Darcy's velocity through media as

$$v = K\tilde{\mathrm{I}} \quad (10)$$

where K is the hydraulic conductivity or proportionality constant and I is the hydraulic gradient. Darcy's velocity can be written as

$$v = \frac{\mathrm{Q}}{\mathrm{A}} \quad (11)$$

where Q is the flow rate and A is the cross-sectional area of the filter that the water travels through, including both the solid and pore area available for flow. Darcy's velocity is not really the average linear velocity since water only travels through the pore spaces. The hydraulic gradient can be written as

$$\tilde{\mathrm{I}} = \frac{\Delta \mathrm{h}}{\mathrm{L}} \quad (12)$$

where ? h is the change in piezometric head and L is the shortest and straight length the water penetrates. In the case of the Filtrón, L is either the bottom or side thickness. L is not the distance the water actually travels because of the pore structure of the filter; the pathway will more likely be in a tortuous or winding path that is not straight. The water travels the real

tortuous path length, not L. Figure 6 illustrates the bottom portion of the filter as an example of the L and A used.

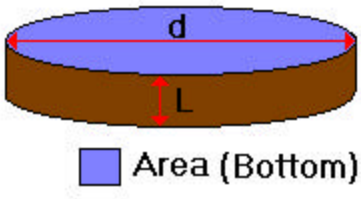


**Figure 8: Cylindrical Bottom Portion of the Filter**

Either calculating or measuring the head before the water enters the media and either measuring or calculating the head after it travels through the filter finds the change in the piezometric head. The difference between the two heads at the two different points will give the change in piezometric head. The piezometric head or commonly referred to as only head is defined as

$$h = \frac{p}{g} + z \qquad (13)$$

where is p is the pressure at the point, ? is the specific weight of the fluid, and z is the physical height of the point in relation to a common datum (same point; for example, the ground). In a nutshell, the head is the energy that drives the fluid to flow from one point to another. If the pressure in Equation 4 is the atmospheric pressure then that part of the equation can be neglected and the head is equal to the z. The version of the Darcy's Equation that will be used in this research is

$$Q = KA\frac{\Delta h}{L} \qquad (14)$$

Darcy's Law is only valid for Laminar flow. In other words, very slow flow which is why it is used most often for groundwater applications including contaminant transport by groundwater.

### 2.9.2 Hydraulic Conductivity

The proportional constant K used in Darcy's Equation is the hydraulic conductivity with the units of length divided by time. Throughout this report there will be many references to hydraulic conductivity and electrical conductivity and they should not be confused with each other. The hydraulic conductivity is found empirically using Darcy's Law while the electrical conductivity is measured directly using an electrical conductivity meter. Seawater, surface water, groundwater, and tap water are types of water that have many ions such $Cl^-$ and $Na^+$ that are not visible to the eye. The more ions that water contains (the higher the ionic strength of the water) the easier the electricity travels through the water; thus, the higher the electrical conductivity of the water. For instance, seawater has a large amount of dissolved salt (NaCl) compared to fresh water and therefore electricity conducts through seawater better then fresh water.

Electrical conductivity has a relationship with electrical conduction while hydraulic conductivity has a similar relationship with how water travels through media. The higher the K value the easier water travels through the media. Table 2 below displays hydraulic conductivity ranges of unconsolidated soil formations as well as their respective particle size ranges:

| Material | Particle size | Hydraulic Conductivity |
|---|---|---|
| Units | mm | m/d |
| Coarse gravel | 16.0-32.0 | 860-8600 |
| Medium gravel | 8.0-16.0 | 20-1000 |
| Coarse sand | 0.5-1.0 | 0.1-860 |
| Medium sand | 0.25-0.5 | 0.1-50 |
| Fine sand | 0.125-0.25 | 0.01-40 |
| Clay | <0.0004 | <0.001 |

**Table 7: Hydraulic Conductivity of Unconsolidated Formations (9)**

The value of K depends on both the characteristics of the porous media and the fluid properties and can be represented by

$$K = \frac{rkg}{m} \qquad (15)$$

where ? is the density of the fluid which depends on temperature; μ is the viscosity of the fluid which also depends on temperature; g is the acceleration due to gravity (9.8 $m/s^2$); and k is the intrinsic permeability ($Length^2$) (8). The intrinsic permeability depends only on the characteristics of the porous matrix such geometry and pore structure of the media or medium, independent of fluid properties (8). In our case, the water is flowing through pores in the ceramic material formed by the combustion away of the sawdust rather than unconsolidated soil grains, but similar principles apply.

### 2.9.3 Tortuosity using Saturated Groundwater Transport Theory

Tortuosity is the term used to describe the twisting and winding of fluid through media. Fluid such as water does not go straight through media as it would in a pipe. It travels through open pores that are connected. I will use the Filtrón as an example to explain this concept, but first some knowledge about the Filtrón construction needs to be discussed.

The Filtróns constructed in Nicaragua use 40% sawdust to 60% clay mixture by volume to make the filters. After the filters are formed, they are placed in a flattop kiln and fired to about 887 $^oC$ resulting in complete combustion of the organic sawdust particles leaving pores within the structure of the clay filter. Some pores are connected and are considered part of the effective porosity of the filter. In other words, the pores that contribute to the pathways for the water to travel through the filter. For the Filtrón, the total general porosity is expected to be about 0.40 because of the sawdust mixture while the effective porosity (*n*) is expected to be less. The effective porosity is expected to be less since not all of the pores will contribute to the pathways for the water to travel. The porosity could be higher if cracks develop in the clay filter (as have been periodically observed) or the clay is not fully compressed prior to firing. Below are the equations defining porosity:

$$\text{General porosity} = \frac{\text{Volume of voids}}{\text{Total volume of the sample}} \qquad (16)$$

$$n = \frac{\text{Void Volume contributing to water pathways}}{\text{Total volume of the sample}} \qquad (17)$$

Figure 7 is an illustration of the situation just discussed, which will lead to the discussion of tortuosity.

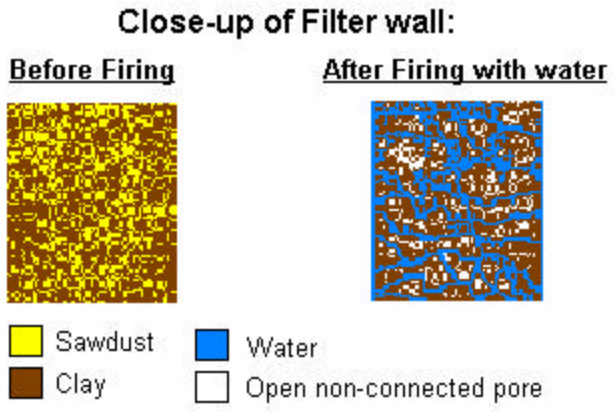


**Figure 9: Microscopic Representation of Filtrón**

Figure 7 is a representation of the microscopic make-up of the filter side wall before and after firing in the kiln. The water was added after the firing to illustrate how there are some open pores that do and do not contribute to the effective porosity. Figure 8 is the zoomed in part of the water saturated schematic in Figure 7.

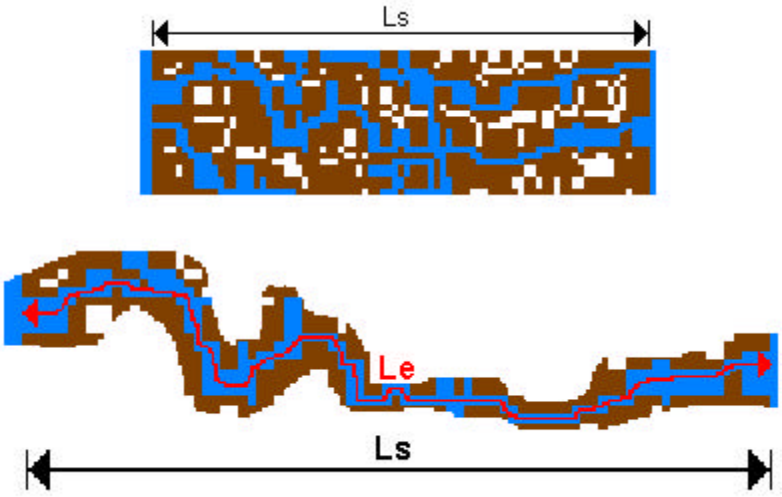


**Figure 10: Magnified Schematic of Water Saturated Side Filter Wall**

Figure 8 illustrates one path that water can take represented by the effective length, Le, in red. Ls is the side length as defined in the Section 2.8 and *L* in Equations 12 and 14. Tortuosity (t) is used to describe the average relationship between Le and Ls in a ratio form as (10):

$$t = \frac{Le}{Ls} \qquad (18)^2$$

[2] Some other references describe t as $(Ls/Le)^2$ but that definition will not be used in this work.

The more tortuous or twisted path water has to take the larger the t factor. The t factor is always greater than or equal to one (10). Tortuosity is usually not measured directly due to difficulty finding the average Le.

The theory used in this research is found in the principles of saturated groundwater contaminant transport in porous media to calculate tortuosity. "There are three basic physical mechanisms by which miscible and immiscible pollutants are transported in the subsurface environment: advection, diffusion, and mechanical dispersion (8)." Mechanical dispersion is the mechanism of solute transport that will be used for this research. This mechanism is "associated both with bulk fluid flow movement and with the presence of the porous medium with its complex, intertwining pore space (8). Fluid particles that are at one time close together tend to move apart because of at least four mechanisms" described by Charbeneau in his text book, *Groundwater Hydraulics and Pollutant Transport* (8):

1. The particles nearest the walls of the pore channel move more slowly than those near the center of the channel.

2. The variations of pore dimensions along the pore axes cause the particles to move at different relative speeds.

3. Adjacent particles in one channel can follow different streamlines that lead to different channels.

4. Differences in the hydraulic conductivity field can allow solute molecules to move at different speeds – even when the hydraulic gradient [I] is uniform.

The resulting transport relative to bulk water movement when these mechanisms occur in the presence of a concentration gradient (difference in concentration of the contaminant or solute) is mechanical dispersion (8). Basically, "dispersion occurs because of our inability to follow the details of pore-to-pore scale groundwater movement (8)." The equation that will be used for this part of the research to represent mechanical dispersion is

$$D = D_m t + a_L v \qquad (19)$$

where D is the dispersion coefficient ($cm^2$/min); $D_m$ is the molecular diffusion coefficient ($cm^2$/min) of the contaminant or for our case Bromide ($Br^-$), the tracer; $a_L$ is the longitudinal dispersivity (cm); and v is the velocity (cm/min) of the water through the pores. The $a_L$*v is the hydrodynamic dispersion coefficient. Hydrodynamic dispersion is when the water flows through the porous medium and differences in velocities within the medium (within a pore and from pore to pore) lead to additional mixing. The longitudinal dispersivity is a property of the porous medium and is related to pore structure.

Similar effects should also occur for pathogen movement through the Filtrón. Additional effects could occur such as sorption, or attachment, to the ceramic pore walls, but such effects will be assumed negligible in this work as a worst-case estimate of pathogen contact time with silver.

### 2.9.4 Previous Studies

Two studies before this one have tried to examine the Filtrón's hydraulic characteristics. The first study was completed by Sten Eriksen (11) in 2001 for Red Cross International. His study was more of a mathematical model for the flow patterns within the Filtrón. Based off of his model, he gave recommendations to Potters for Peace. His model was then reevaluated by Daniele Lantagne of Alethia Environmental in a section of *Report 1: Intrinsic Effectiveness,* which is the second study that examined the Filtón's hydrodynamic characteristics.

#### 2.9.4.1 Eriksen's Model

This section is my interpretation of Eriksen's mathematical model and analysis of the Filtrón. Eriksen used a cylindrical geometric shape of the average conical filter diameter to represent the Filtrón and used Darcy's Law for the flow. His mathematical model is for the flow once the filter is completely full with water and no water is added once the filter starts operating. In other words, the water level inside the Filtrón is decreasing with time as the filter operates. His main three assumptions for the flow are:

1. The hydraulic conductivity for the bottom and sides of the filter are the same.

2. The head driving the flow through the filter's sides and the bottom of the filter are the same when using Darcy's Law.

3. The maximum velocity of the water is through the bottom with the when the filter is completely full.

Table 3 below defines the parameters Eriksen used for his model followed by the equations he used to model the flow.

| Parameter | Definition |
|---|---|
| **$Q_s$** | Flow rate through the side of the filter |
| **$Q_b$** | Flow rate through the bottom of the filter |
| **k** | Hydraulic conductivity of the filter |
| **a** | Thickness of the side |
| **b** | Thickness of the bottom |
| **z** | Variable height of the water inside the filter used in his integration |
| **x** | Height of the water inside the filter |
| **H** | Maximum height of water inside the filter |
| **D** | Average diameter of the top and bottom diameters |

**Table 8: Eriksen Model Parameter Definitions**

$$Q_s = \int_0^x \frac{kpDz}{a}\,dz = \frac{kpDx^2}{2a} \qquad (20)$$

$$Q_b = \frac{kpD^2x}{4b} \qquad (21)$$

Using the total flow ($Q_s$ plus $Q_b$) he derived an equation that would give the average time it took for the water to travel through the filter based on the initial height of the water inside the filter and the final height of the water. He calculated this so that he could determine the maximum allowable hydraulic conductivity of the filter. See Appendix A for my rederivation of his time equation. Equation 22 is the equation he derived, which is simplified slightly differently than my derivation; however both variations result in the same numerical answer when the same numbers for the parameters are used.

$$T = \frac{b}{k}\ln\left[\frac{H(1+l(\%_H))}{x(1+l)}\right] \qquad (22)$$

$$l = \frac{2bH}{aD} \qquad (23)$$

Using Equation 22, Eriksen determined the maximum hydraulic conductivity that would allow for an average of 25 minutes of exposure time with the colloidal silver in the filter. At this time, the percentages of inactivation for bacteria, pathogenic viruses, and pathogenic protozoan with the 25 minute contact time and an exact concentration (unknown what he is assuming) are unknown. Therefore, 25 minutes of contact time provides an unknown percentage of inactivation of different specific pathogens. Eriksen's conclusion was that the filter should be used "in connection with post chlorination [sic] and without colloid silver (11)." He concluded this for two reasons – (1) "the filter is easier to clean than a sand filter [which I assume he was comparing it to] and [is] more uniform (11)" and (2) the actual hydraulic conductivity was 1000 times greater than the allowable conductivity to achieve sufficient contact time for adequate pathogen removal/inactivation (assuming 25 minutes is needed).

**2.9.4.2 Alethia Environmental Reevaluation**

In Lantagne's work, the experimental pathogen inactivation achieved was significantly greater than predicted by Eriksen. Therefore, Daniele Lantagne reevaluated the Eriksen mathematical model in Section 5.1.2 of *Report 1: Intrinsic Effectiveness* (3). In that section, she explained his model and improved some of his values that he used with the model. She stated, "two values that Eriksen used in his equations to determine the actual and maximum values of hydraulic conductivity were not ideal (3)." Her first improvement was in the calculation of the maximum allowable hydraulic conductivity to allow 25 minutes of contact time with colloidal silver and her second improvement was the calculation of the actual hydraulic conductivity of the filter.

Eriksen determined that the minimum time needed for bacterial inactivation would be the distance the water traveled through the colloidal silver layer divided by the velocity, which is represented by

$$T_{\min} = \frac{cb}{kH} \qquad (24)$$

where *kH/b* (Darcy's Law) is the maximum velocity through the bottom of the filter when the filter is full; *c* is the thickness of the colloidal layer; and the other parameters were defined in the previous section. Rearranging the equation while solving for *k* led to

$$k_{max} = \frac{cb}{T_{min} H} \qquad (25)$$

Figure 9 is a representation of Eriksen's colloidal silver layer presumption of only a thin surface layer film. The background in the picture is dark so that the colloidal silver layer can be easily seen. The figure is not to scale.

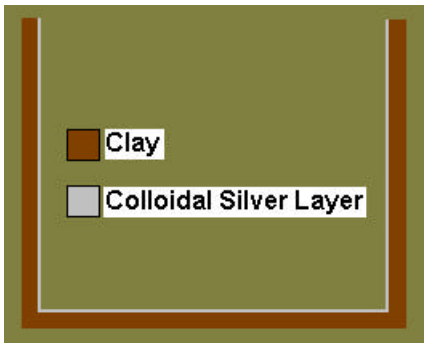


**Figure 11: Eriksen Colloidal Silver Layer Representation**

Ms. Lantagne updated the thickness of the colloidal silver using tortuosity; her first improvement of Eriksen's model. Eriksen used 0.1 mm for the colloidal silver thickness because he said it was the value "according to the paper by Earp (11)." The actual colloidal silver layer thickness at this time is unknown; however at the minimum there is at least 0.2 mm using Eriksen's logic. The colloidal silver during construction is painted on both sides of the filter and the silver layer is not visible to the human eye. The silver seeps into the pores of the filter, and the distance it seeps into the pores is probably greater than 0.1 mm.

Eriksen did not consider the path taken by the water; hence he did not consider tortuosity. In his model, he assumed that the bacteria were only exposed to the colloidal silver in the first 0.1 mm of the filter. Daniele stated in her report, "the appropriate thickness here is the thickness of the colloidal silver layer coating the pores in the ceramic through which the bacteria comes into contact with the colloidal silver (3)." Below is an illustration of her statement:

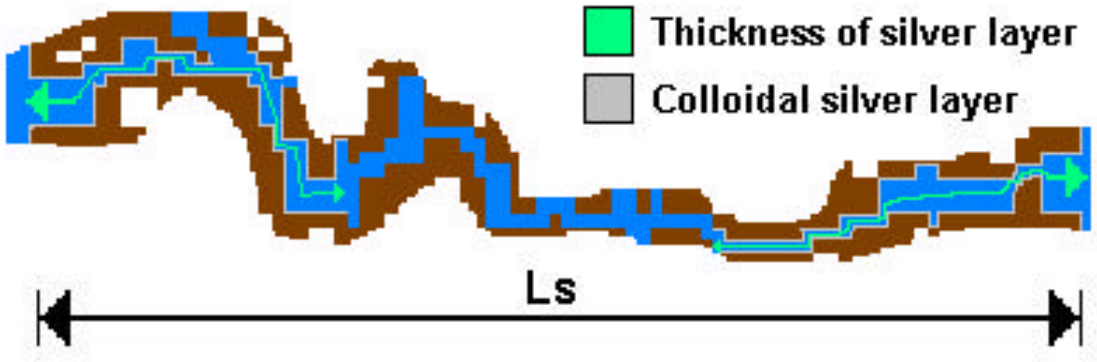


**Figure 12: Colloidal Silver Layer Thickness Illustration in the Pores**

Daniele improved the colloidal silver thickness from Eriksen's 0.1 mm estimate to 4 mm. She assumed that the thickness of the layer on both sides was at least 1 mm each resulting in a thickness of 2 mm. This was only an estimate and she recommended further analysis of the

silver layer thickness. She then multiplied the thickness by a tortuosity factor of 2 for a total of 4 mm, which was only an estimate assuming that the average length of the water path is twice as long as the thickness of the filter (Ls in Figure 10).

The second value improvement of Eriksen's study by Lantagne was the actual hydraulic conductivity value based on the time needed for the filter to empty. According to Lantagne, "Eriksen referenced Ron Rivera as stating [that] the filter takes one to two hours to empty completely (3)." Eriksen must have misunderstood Rivera because the flow rate of the filter is 1 to 2 Liters per hour and a test completed by the University of Nicaragua showed that the filter empties completely in approximately 7 to 9 hours. Lantagne's testing in the United States confirmed that the longer time to completely empty the filter was correct (3).

Eriksen used the misunderstood information about the flow and made assumptions for Equation 22 to calculate the actual hydraulic conductivity. The time used for Eriksen's model was 1 hour for the filter to completely empty while Lantagne used 8 hours.

Below is a summary table of the numbers used for the Eriksen model and the numbers used for Lantagne's improvements of his model with the results of the calculated maximum and actual hydraulic conductivities.

| Parameters | Eriksen | Lantagne |
|---|---|---|
| **Equation 25** | $k_{max} = \frac{cb}{T_{min} H}$ | |
| **c** | 0.0001 m | 0.004 m |
| **b** | 0.010 m | 0.010 m |
| **$T_{min}$** | 25 min | 25 min |
| **H** | 0.240 m | 0.240 m |
| **$k_{max}$ (Results)** | 0.00001 m/hr | 0.0004 m/hr |
| **Simplified Equation 22** | $k_{actual} = \frac{b}{T} \ln\left[\frac{H}{x\left(1+\frac{2H}{D}\right)}\right]$ | |
| **b** | a = b | a = b |
| **T** | 1 hour | 8 hours |
| **H** | 0.240 m | 0.240 m |
| **D** | 0.200 m | 0.200 m |
| **H/x** | 100 | 100 |
| **$k_{actual}$ (Results)** | 0.03 m/hr | 0.004 m/hr |

**Table 9: Mathematical Parameters and Calculated Results of Previous Studies**

Eriksen concluded that because the actual hydraulic conductivity (0.03 m/hr) was 1000 times larger than the maximum hydraulic conductivity (0.00001 m/hr) the colloidal silver was ineffective in the Filtrón for microbial reduction. When Lantagne improved his mathematical

model with more accurate estimates for the thickness of the colloidal silver layer and time for complete drainage of a filter, the difference between the actual and maximum hydraulic conductivity was only 10. She concluded that Eriksen's conclusion about the ineffective colloidal silver "is not held up once updated values are used in the equations" he derived (3).

Lantagne acknowledged that her estimate of the colloidal silver thickness was a "very rough estimate" and it "needs additional laboratory analysis to verify the accuracy" (3). She ended her reevaluation of the Eriksen Model by highly recommending "that further research using the framework of Eriksen's model be completed" (3).

### 2.9.5 Model Comparison

The purpose of this section is to compare my mathematical model with the Eriksen Model already discussed.

Daniele Lantagne credited Sten Eriksen with his mathematical model as "mathematically sound and very powerful" (3). He made assumptions that I feel are not completely valid for such a geometrically complex and unconventional filter. There are four fundamental differences between his model and mine starting with the geometric shape and ending with the flow through the sides.

#### 2.9.5.1 Geometric Shape Difference

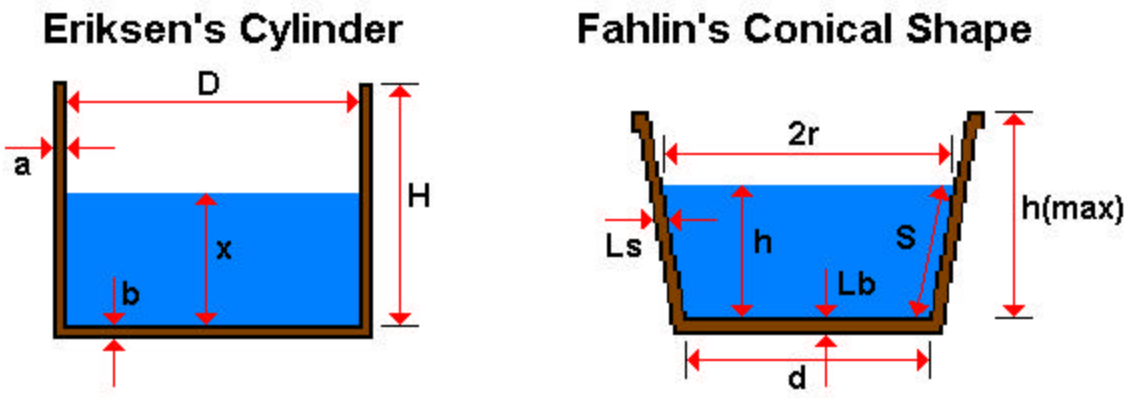


**Figure 13: Eriksen and Fahlin Geometric Models Comparison**

Figure 11 illustrates the differences in the geometric shapes and the different nomenclature for the parameters of the filter. Figure 11 is not to scale but the two models are similar to the proportions between the two models. For instance, Eriksen's side and bottom have the same thickness and the thicknesses in my model are different and larger (as verified by measurement of the 5 Filtróns as described later in Section 4.2). In addition, Eriksen's diameter (D) is the average diameter of the Filtrón while my model reflects the actual diameter difference between the top and bottom circles. Furthermore, the maximum height of the filter is longer in the Eriksen Model than the Fahlin Model (again, measured from real Filtróns).

By using the average diameter (D), Eriksen's bottom area is 40% larger then the actual bottom area of the filter. In addition, by using D and H, the maximum height of the water for the

Eriksen model (24 cm), the volume is about 18% larger then the actual volume contained inside the filter.

When calculating hydraulic conductivities, these differences in area and volume can make a significant difference. My model represents the true shape and size of the Filtrón while Eriksen's Model is an over simplified version of the same filter.

**2.9.5.2 Hydraulic Conductivity Difference**

Eriksen assumed that the hydraulic conductivities of the bottom and sides were the same. I am assuming that the hydraulic conductivities are different for one reason. During the construction of the filters, a bulk piece of mixed clay and sawdust about the size of a cantaloupe ready to form is put into the bottom part of the mold to be pressed. The mold is made of two separate parts – the top and bottom. As the top part of the aluminum mold is pressed, the clay and sawdust "cantaloupe" is forced to travel up the slanted sides of the mold to the top where the excess clay and sawdust is removed. Most of the compression force is exerted vertically on the bottom while the sides are not subject to the same type and quantity of force, which is why I assumed the hydraulic conductivities for the bottom and sides are different.

I assumed the hydraulic conductivity on the bottom ($K_b$) was less then the hydraulic conductivity of the side ($K_s$). This assumption is based on the notion that since the bottom was compressed more the pore sizes are smaller and possibly more tortuous.

**2.9.5.3 Head Difference**

In my interpretation of Eriksen's application using Darcy's Law, he assumed that the head driving the water through the bottom was the same as the head driving the water through the side. As defined by Equation 4 in the theory section, the head is the vertical distance ($z$) driving the water through the filter since the pressure in Equation 4 is atmospheric. Using Eriksen's logic, the head at every point on the surface of the side was the same regardless of the elevation on the surface. In other words, the head driving the water through the side surface was uniform and equal to the head forcing the water through the bottom.

My model shows that the head is not uniform. Figure 12 on the next page is a representation of the non-uniform head distribution on the side and the maximum head forcing the water through the bottom of a full Filtrón.

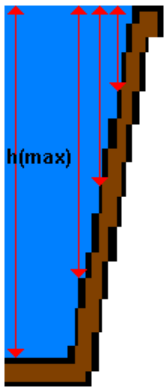


**Figure 14: Head Distribution in the Fahlin Model for One Side of the Filter**

Eriksen's side head assumption might have been true only if the water paths inside the side wall were connected vertically with atmospheric pressure at the top of the column and this column of water traveled out the side bottom of the filter. This is not a possibility since inspection of the filter while it is operating during my experiments and Lantagne's (3) show that the water drips out of all elevations on the outer surface of the filter sides. The head is not uniform or constant at every point.

I did not know how to accurately model the non-uniform flow on the side, but I did attempt to model it by two methods – a lumped $K_s$' parameter for the side hydraulic conductivity times side head and a side head factor. Using Darcy's Law, I lumped $K_s$ and the side head ($h_s$) in one parameter $K_s$'. The drawback to this was that as the head for the side changed, the real $K_s$ (side hydraulic conductivity) remained constant. Therefore, the resulting $K_s$' number is more of an average of the two for all water levels within the filter. During an individual constant flow test, this effect is not significant since the water volume in the Filtrón remained constant. The second method, or side factor method, consisted of using the factor *F* times the vertical head, $h_b$, to represent the side head. I assumed that the *F* factor was constant. The *F* factor is a number between zero and one, which represents the fraction of the vertical head that is experienced at the side of the filter. Equation (26) is the equation for the side head using the *F* factor.

$$h_s = Fh_b \qquad (26)$$

### 2.9.5.4 Flow through the Sides Difference

Since the hydraulic conductivity and side head assumptions are different, definitely the numerical value for the flow through the side will be different; however, there is one more reason for more of a difference between the two models.

Eriksen's side flow, $Q_s$, was integrated with respect to the height of the water inside the filter because he wanted to model the average side flow as the filter emptied. I did not integrate with respect to the water level in the filter because for my experiments I maintained a constant flow using a pump, which resulted in a constant water level in the filter. From this constant behavior, I will be able to get a more accurate representation of the flow that is not averaged.

Equation 27 is the ideal application of Darcy's Equation provided that $h_s$ is known. Equation 26 will be plugged into Equation 27 since $h_s$ is not known. Equation 28 is Darcy's Equation as well using the lumped $K_s$' parameter. ($Q_T = Q_b + Q_s$)

$$Q_T = \frac{K_b A_b h_b}{L_b} + \frac{K_s S A_1 h_s}{L_s} \tag{27}$$

$$Q_T = \frac{K_b A_b h_b}{L_b} + \frac{K_s' S A_1}{L_s} \tag{28}$$

There is one similarity with Eriksen's and my model – the application of Darcy's Equation for the bottom flow. With the exception of the different hydraulic conductivity assumption and different values from our geometric models, we modeled the bottom flow the same.

## Section 3.0 Methods

### 3.1 Experimental Methods

The experimental methods used in this research are divided into two phases – (1) Hydraulic Conductivity Tests and (2) Bromide Tracer Breakthrough Tests. Each of these sections will describe the variables and parameters measured and methods such that they can be replicated in the future. But first, it is important to understand the physical set-up of the experiments in the lab.

#### 3.1.1 Laboratory Set-up

Each filter was placed in a standard five gallon plastic bucket, or receptacle as Potters for Peace prefers to call it. I purchased the receptacles from Home Depot® and the filters fit extremely well. Potters for Peace designed the filters to have that capability and 5-gallon plastic buckets seem to have a uniform size and geometry worldwide at least in the US, Nicaragua, and Belize. The approximate dimensions of the receptacle are 14.25 inches high with a diameter of 11.50 inches. At the bottom center of the each receptacle, I drilled a hole and placed a plastic fitting in the hole and sealed it with silicon. This enabled me to connect $^1/_2$ inch, fixed piping with a ball valve at the end. From the end of the fixed piping, a clear, flexible hose was attached and led to a drainage area, or large sink. When the units are used in homes, a spigot is attached at the side of the receptacle near the bottom, but this increases the water volume retained inside the receptacle before the water leaves. Therefore, the side spigot was not optimal for these experiments.

For the input water, each filter had a plastic tube that dripped water into the filter from the deionized water faucet in the lab. This water is the city of Boulder's tap water that is passed through US Filter resins to remove exchangeable ions and then an activated carbon filter to further reduce organics. Over time of water treatment, the resins and activated carbon becomes "exhausted" and must be replaced. This is indicated by a light that shows when electric conductivity of the water is too high. Resin replacement occurred on 3 and 25 October and 6 November during my experiments. Two resins were replaced on 3 October.

The water was pumped at a fairly constant flow rate per trial using a Masterflex® peristaltic pump and Tygon® 13 and 16 tubing inner diameter 0.8 and 3.1 mm, respectively (outer diameter 4 mm to 6.5 mm, respectively). The deionized water used was not the best possible water quality, although it was good water to use because it did not have suspended solids to contribute to clogging. It did, however, contain a low amount of organic carbon. The measured amount of total organic carbon (TOC) was 96 parts per billion (ppb) +/- 4, which is extremely low compared to regular tap water. Boulder's tap water typically has about 1000 ppb (1 ppm) of TOC (12). Raw water typically treated in a Filtrón being used internationally likely contains 1 to 20 mg of carbon per liter for surface water and 0.1 to 2 mg of carbon per liter for groundwater (1 – 20 ppm and 0.1 to 2 ppm of carbon, respectively) (13). The TOC was only measured once in the middle of November so I cannot say if it varied considerably or remained constant. I only measured it once because I was having some potential clogging (loading) issues that I could not explain.

The purpose of using deionized water versus tap or untreated water was to get an accurate idea of how water optimally travels through the filter without loading, i.e. solids and/or biological clogging. The less the water has other substances the better the test results would be because there would be minimal nutrients for microorganisms. Milli-Q® water was not used because of the large volume required for the experiment and the limited resources of Milli-Q® water in the lab. Milli-Q® water is a brand name of laboratory water that is basically deionized water with added membrane filtration such as reverse osmosis to produce ultra-pure water. There are only trace levels of anything other than the pure water. The deionized water used was the most abundant and easily accessible high quality treated water.
Below is a schematic of the set-up from the source to the outflow:

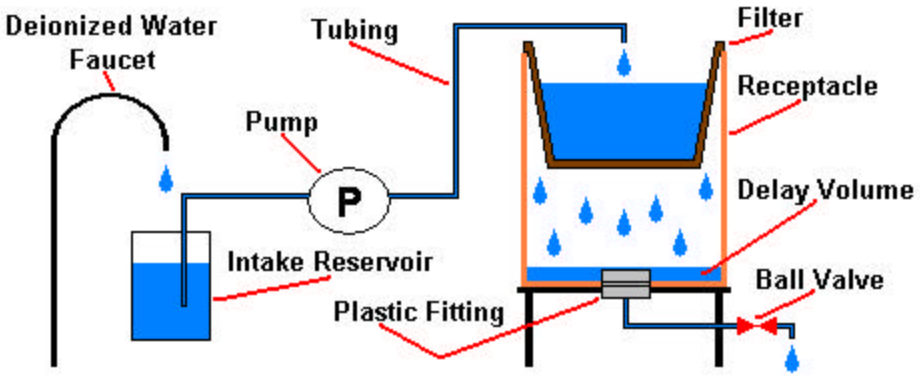


**Figure 15: Physical Set-up Schematic in the Lab**

Figure 13 illustrates the delay volume created by the plastic fitting in the receptacle. The water does not immediately flow from the filter to the exit piping; there is some delay, but this volume is accounted for in analysis of the Bromide tracer breakthrough test results. The volume is equal to 1050 mL and it is called the "delay volume." Delay due to the travel time in the tubing from the reservoir to the filter is negligible, as the total tubing volume ranged from 4 to 6 mL. Therefore, with flow rates from 10 to 45 mL/min the tubing delay was less than one minute. The "delay volume" has no effect on the hydraulic conductivity tests. The set-up presented in this section is exactly how the water travels during the Hydraulic Conductivity Tests.

### 3.1.2 Hydraulic Conductivity Tests

The purpose of these tests is to calculate $K_b$ and $K_s$, hydraulic conductivity through the filter bottom and the hydraulic conductivity of the filter side. The influent flow rate, *Q*, varied from as low as 5 mL/min to as high as 40 mL/min. Q was controlled by the peristaltic pump. Each filter was tested at a minimum of eight different Q values. At each flow rate after the filter had reached steady state, the height of the water in the center of the filter (*h*) and the length of the water on the side (*S*) were measured using a ruler with 1 mm increments. I assumed the flow rate out of the filter was equal to the flow rate in once the filter had reached steady state. Steady state was assumed after the filter had been running for at least 4.5 to 5 hours. At steady state the water volume in the Filtrón should be constant; thus, the measured *h* and *S* should be constant. Each of the filters was tested. The parameters *h* and *S* were measured at least three times over a minimum of 24 hours. The calculations for $K_b$ and $K_s$ will be addressed in the numerical methods section for hydraulic conductivity (Section 3.3.1).

### 3.1.3 Bromide Tracer Breakthrough Tests

The purpose of these tests is to calculate the tortuosity factor by solving for the dispersion coefficient, side porosity, and bottom porosity. This was accomplished by measuring the electrical conductivity of the water as it passed through the filter at various time increments after switching from clean deionized water to bromide spiked deionized water. With the data collected and plotted, I could determine the time at which the Bromide tracer initially "broke through" and when 50% of the tracer concentration "broke through." This would correspond to the minimum and average pathogen contact time in the ceramic wall of the Filtrón. The calculation of the tortuosity factor will be discussed in the numerical methods section for the Bromide tracer breakthrough tests.

The physical set-up presented in the Section 3.1.1 is exactly how the water travels during this test except that the source is not deionized water from that faucet. The source water was from another deionized water tap that was closer to ideally deionized water, which I will call "improved deionized water." The electrical conductivity of fully deionized water should be about zero micro-Siemens (µS) and the "improved deionized water" was equal to 0.5 ± 0.1 µS while the regular deionized water ranged from 4 to 6 µS. The "improved deionized water" was poured into a 117 Liter container (plastic trash can) and it was pumped from the container to the intake reservoir shown in Figure 13 using a submerged pump.

Before the tracer test began, the "improved deionized water" was fed to the filters until they reached steady state. By reaching steady state, at least one complete volume of water contained in the filter had filtered through the water displacing any water that was previously in the filter. In other words, I had to make sure that the water from the previous test had completely traveled through the filter before the test could begin. The time it takes for one volume to go through the filter is also called residence time or retention time. Below is the calculation of the residence time I used as the steady state guideline:

$$t = \frac{V}{Q} \Rightarrow \frac{8000\ \text{mL}}{30\ \text{mL}/\text{min}} = 267\ \text{minutes} \approx 4.5\ \text{hours}$$

8000 mL was used for the filter volume since most of the five filters had their measured volumes near that number (See Table 10: Calculation Summary of the Filters). This approximation does neglect the volume of water in the pores of the ceramic filter.

After the filter had reached steady state, I dissolved about 5 grams of solid potassium bromide in the 117 Liter container. This resulted in a electrical conductivity of about 60 µS. I measured the conductivity of the flow out of the filters before I started pumping the bromide spiked water into the intake reservoir to establish a baseline conductivity. To measure the conductivity of the water, I used an electrical conductivity meter (Hanna Instrument) with ±0.1 precision over a 0 to 199.9 µS range and a minimum detection limit of 0.1 µS. The instrument was calibrated for each run of the experiment and the raw data was corrected for this calibration (See Appendix B for the method). As soon as I started pumping the tracer-spiked water, the clock started and the time was set to zero. I measured the conductivity of the effluent from the receptacle under each filter at various time increments ranging from every 10 minutes to every hour depending on the test. The conductivity of the water increased due to the concentration of the bromide.

Each filter was tested at a high, medium, and low flow rate. Table 5 below summarizes for each of the filters their serial numbers and their respective flow rates:

| **Filters** (* no silver) | **1** | **2** | **3** | **4** | **5*** |
|---|---|---|---|---|---|
| **Serial numbers** | 18004 | 19499 | 18036 | 17945 | 18193 |
| **Units** | mL/min | mL/min | mL/min | mL/min | mL/min |
| **High Q** | 32.3 | 45.6 | 35.3 | 23.2 | 33.7 |
| **Medium Q** | 19.1 | 20.9 | 21.0 | 10.6 | 20.0 |
| **Low Q** | 14.6 | 14.9 | 16.1 | 5.6 | 13.5 |

**Table 10: Flow rates for the Bromide Tracer Breakthrough Tests**

### 3.2 Observations during the Tests

Two phenomena were observed during the experimental process – "wicking" and loading. The "wicking" phenomenon describes the water saturation of the filter once water is added to an unsaturated filter. As the water is added to a dry or unsaturated filter, I could observe that the water traveled vertically to the height of the water in the filter by the darkening of the filter. Not much water would start flowing until the entire filter was the darker color or more saturated including the lip used to support the filter in the receptacle. Independent of the height of the water inside the filter the regions above it remained saturated, probably due to capillary action. Webster defines the second meaning of wick as "to carry (as moisture) by capillary action" hence the use of the word to describe the phenomenon (14). It must be noted that this wicking may change the true "volume" and/or "area" of the ceramic filter through which the water is moving. This real area and/or volume is greater than or equal to "free" internal water volume and may lead to errors in Eriksen and Fahlin equations to model water flow through the filter.

During Phase One, there was some unexpected loading of the filters that affected the results because of the potential clogging it caused. Loading is the increasing accumulation of mass as the filters operated. All of the filters, except Filter 4, experienced the same loading phenomena. Possibilities for the loading will be discussed in Section 4.0 Results, which are briefly stated below:

1. Deionized water source quality slightly decreased over time

2. Biological growth not visible to the human eye occurred in the tubing and/or in the Filtrón itself

3. Colloidal silver contact sites were covered by some substance or combination of substances

### 3.3 Numerical Methods

Microsoft Excel® was used for the numerical analysis of the data from the Hydraulic Conductivity and Bromide Tracer Breakthrough tests. The Solver used for the Hydraulic Conductivity and Bromide Tracer Breakthrough Tests is the Premium Solver for Education – an upgraded version of the standard Solver that is in Excel®. The type of Premium Solver used is the Standard Evolutionary. This type uses Evolutionary (or genetic) algorithms inspired by Darwin's theory of evolution and created by researchers interested in mathematical optimization.

It is a powerful general-purpose optimization engine that generally does not get trapped at a local optimal solution.

### 3.3.1 Hydraulic Conductivity Numerical Methods

This method involves plotting, eliminating not essential data, using the trendline capability, and using the Standard Evolutionary Solver. First, all the data was plotted for each filter by comparing the Surface Area 1 ($SA_1$), which is the side surface area, versus the flow rate, $Q_{in}$. I anticipated a linear relationship (as the flow rate increased so would the side surface area) assuming the hydraulic conductivities would remain constant but not necessarily for the side and bottom over all experiments. As mentioned in the previous section, the loading phenomena caused a problem I could not directly explain. The results were not as linear as expected so I had to eliminate inconsistent or outlying data. I only evaluated the data that had a relatively linear relationship.

The data was evaluated by two approaches and each approach was done twice with two different equations to represent the flow. The first approach was to use the measured data and the second approach was to use a line obtained from the data.

#### 3.3.1.1 Measured Data Approach

Equations 27 and 28 from the theory section were used to represent the flow through the filter. Both of the equations' variables were solved for using Excel®. Using the linear data measured, a table of at least eight data points over the flow rate range was set-up. Both equations had their own table. Table 6 is an example of the table used for each filter; it is from Filter 1's spreadsheet.

| | Q | h | S | Lb | Ls | r(h) | SA | SA1 | Ab |
|---|---|---|---|---|---|---|---|---|---|
| Points | mL/min | cm | cm | cm | cm | cm | $cm^2$ | $cm^2$ | $cm^2$ |
| Certainty | ±0.2 | ±0.1 | ±0.1 | ±0.1 | ±0.003 | ±0.1 | ±24 | ±12 | ±2 |
| 1 | 10.0 | 8.7 | 9.0 | 1.5 | 1.252 | 10.8 | 2210 | 564 | 272 |
| 2 | 14.7 | 10.8 | 11.1 | 1.5 | 1.252 | 11.1 | 2353 | 7074 | 272 |
| 3 | 7.8 | 6.3 | 6.5 | 1.5 | 1.252 | 10.4 | 2046 | 4004 | 272 |
| 4 | 6.7 | 5.2 | 5.4 | 1.5 | 1.252 | 10.2 | 1973 | 327 | 272 |
| 5 | 17.9 | 14.6 | 14.9 | 1.5 | 1.252 | 11.7 | 2628 | 982 | 272 |
| 6 | 21.0 | 17.4 | 17.8 | 1.5 | 1.252 | 12.2 | 2844 | 1198 | 272 |
| 7 | 25.6 | 19.9 | 20.3 | 1.5 | 1.252 | 12.6 | 3041 | 1395 | 272 |
| 8 | 13.7 | 15.6 | 16.0 | 1.5 | 1.252 | 11.9 | 2707 | 1061 | 272 |
| 9 | 27.5 | 20.3 | 20.8 | 1.5 | 1.252 | 12.7 | 3077 | 1431 | 272 |

**Table 11: Filter 1 Example Table for the Measured Data Approach**

Columns Q through Ls were measured values while the remaining columns were calculated. Q was measured by using a 10 mL graduate cylinder (0.1 mL gradations) and a stop watch (0.01 sec precision). The parameters h, S, and Lb were measured with a standard ruler (1 mm gradations). Ls was measured using a caliper that had a precision of ten hundred thousandths of an inch (±0.003 cm). Furthermore, Ls was measured at 8 different positions around the filter at about 2.5 inches from the top (the calipers could only go down so far). The eight different measurements were averaged for the value in the Ls column.

The certainty row in Table 6 has a plus and minus sign in front of a number to indicate the range of the actual value. For instance, the first row's flow was 10.0 mL/min with 0.2 mL/min certainty. The range of the actual flow is 9.8 to 10.2 mL/min, which is reasonably accurate to 10.0 as the measurement. The certainties from the measured values were used to calculate the certainties of the calculated values (r, SA, SA1, and Ab).

Once the table was set-up for each filter, three additional columns were added to the right. First, Equation (28) was used for the equation representing the overall flow. The first column was the flow through the bottom ($Q_b$) for each point as discussed in the theory section. The second column was the flow through the side ($Q_s$) for each point. The third column was used to sum each point with the actual flow ($Q_T$) minus $Q_s$ plus $Q_b$ and square it. At the bottom of the third column was total sum cell for that column, summing all the squared differences. This total sum cell was the cell that was minimized using the evolutionary solver.

Solver requires a cell to be maximized, to be minimized, or set to certain value by changing a few cells within given constraints. Because I used the Premium Solver for Education, I had the option to choose one of the three solvers available (a linear, non-linear, and evolutionary) and as previously mentioned I selected the Standard Evolutionary Solver.

Once the total squared difference cell was selected to be minimized, the changing cells were selected and the constraints were input. Since Equation (28) was used, the changing cells were $K_b$ and $K'_s$. The following are the constraints input:

$$K_b = K'_s$$

$$K_b \text{ and } K'_s = 0.00001 \text{ cm/min}$$

$$K_b \text{ and } K'_s = 0.1 \text{ cm/min}$$

$K_b$ was assumed to be less than or equal to $K'_s$ because the side head is included in the $K'_s$ variable. $K_s * h_s = K_s'$, and $h_s$ was greater than or equal to 1 cm for all experiments. $K_b$ and $K'_s$ are greater than or equal to 0.00001 and less then or equal to 0.1 because $K_b$ and $K'_s$ cannot be negative and larger than 0.1. Initially, the $K_b$ and $K'_s$ were set to 0.1 for the initial guess to be used for the solver and the total flow results before the solver ran showed that 0.1 was too high, but would be a decent place to start. The solve button was pressed once the cell to be minimized was chosen, the changing cells selected, the constraints input, and the initial guess established. The results were output once the solver had completed its process.

Equation (27) was the second equation used for this type of method using the measured data. The only difference in this method from using Equation (28) was the addition of a changing cell, F (the factor times the vertical head, *h*, to equal $h_s$, the side head), and the addition of three constraints. $K'_s$ was now $K_s$ because the side head ($h_s = F h_b$) was not included in the side hydraulic conductivity. The three additional constraints are inputted below and on the next page:

$$F = 1$$

$$F = 0.00001$$

$$Q_b = Q_s$$

The side head cannot exceed the vertical head and the factor, F, cannot be negative. Based on the painted results from Daniele Lantagne's investigation, more water flowed through the side than the bottom. In her investigation, a filter was painted on the sides with impermeable paint to stop water flow through the side and another filter was painted on the bottom with the same paint to measure the water flow through the side. Both filters had the same flow rates before they were painted. She found $Q_s$ equal to 1.04 liters per hour, and $Q_b$ equal to 0.21 liters per hour, for a total flow rate of 1.25 liters per hour which was lower then the overall flow before being painted implying a synergistic effective between the bottom and sides of the filter (3). From her results, the above constraint ($Q_b = Q_s$) is justified.

The next step is the same as using Equation (27). Once the cell to be minimized was chosen, the changing cells were selected, the constraints input, and the initial guess established (same as before). The results were output once the solver had completed its process. The following figures show the convergence settings used with the solver:

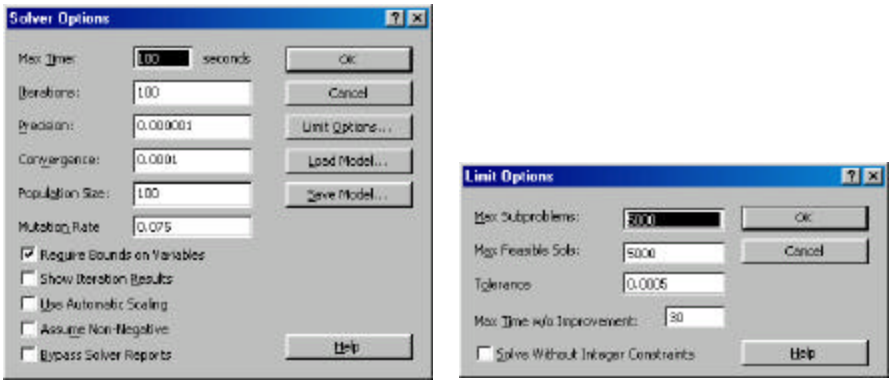


**Figure 16: Convergence, Precision, and Limits for the Evolutionary Solver**

The results using this equation were not as useful as the results using Equation (28). The method just described was used for the data measured, the next section is about how the ideal points could be used for this same process.

### 3.3.1.2 Points from Line Approach

The main difference between this approach and the measured data approach is the points that were used to do the same solver method.

After the raw data was selected, I used the linear trendline capability in Excel® to fit the raw data to a line. From the trendline, I was able to use a linear equation to represent the relationship between Q and $SA_1$. From the linear relationship, I solved for the height of the water, *h*, in the filter for at least 8 points on the line using the quadratic equation. As stated is the measured data approach, each point from the line had its own sum cell in Excel®. All of the sum cells for each filter were added to together for a total sum cell. Again, this cell is what solver tried to minimize. The exact same method using Excel® and the Standard Evolutionary Solver as in the measured data approach section was utilized for both Equations 27 and 28.

### 3.3.2 Bromide Tracer Breakthrough Numerical Methods

The purpose of these methods is to calculate the tortuosity factor for each filter for each level of flow (high, medium, low) by using saturated groundwater transport theory. If the tortuosity of the pores in the bottom and all along the sides of the filter were constant, the same tortuosity factor should fit all three experiments for each filter. This was not really expected, but could provide a good average tortuosity given a more robust data set. The electrical conductivity of the water exiting each filter was measured at certain time (10 to 90 minute) increments for an extended period of time (minimum 500 minutes to maximum 1200 minutes). The standard curve was used to convert measured electrical conductivity (µS) to actual, and baseline conductivity was corrected out. The data was plotted as Bromide concentration versus time. From the plotted data, the theory was used to model the behavior of the filters by solving for the unknowns – side porosity, bottom porosity, and dispersion coefficient. Once the unknowns were solved using the Standard Evolutionary solver in Excel®, the dispersion coefficient was used with longitudinal dispersivity, velocity of the water, and the molecular diffusion of Bromide to solve for the tortuosity. This section is broken into subsections to easily present this complicated method for calculating tortuosity.

#### 3.3.2.1 Definition of Model for Data

Each data point was compared to a calculated value or modeled originating from two equations. The equations originated from the theory of saturated groundwater transport as presented in Fetter (1999) and the equations are a simplified version. Modeling the data to get the calculated value I used two situations.

If U<1,

$$C = \frac{C_o}{2} erfc\left[\frac{1-U}{\sqrt{\frac{2UD}{vL_w}}}\right] \qquad (29)$$

If U>1,

$$C = C_o - \frac{C_o}{2} erfc\left[\frac{U-1}{\sqrt{\frac{2UD}{vL_w}}}\right] \qquad (30)$$

where C is the concentration, $C_o$ is the initial concentration, U is a unitless number, D is the dispersion coefficient as mentioned in the theory section, v is the velocity of the water, and $L_w$ is the weighted length. Since the conductivity was proportional to concentration of the Bromide tracer, C and $C_o$ were actually the electrical conductivity of the water in micro-Siemens (µS). U is defined on the next page.

$$U = \frac{Qt}{V_1 + V_u + V_b} \qquad (32)$$

In the experiments, *U* was initially less than one and then became greater than one as time increased. Table 7 below defines the variables in the above equation:

| Variable | Units | Definition |
|---|---|---|
| Q | mL/min | Flow rate of water through the filter |
| t | minutes | Time of conductivity measurement |
| $V_1$ | mL | Volume of water within the filter |
| $V_u$ | mL | Volume of water in the pores of the filter that is estimated |
| $V_r$ | mL | Constant volume of water in the receptacle (1050 mL) |
| $A_H$ | $cm^2$ | Area of the bottom triangle not included in the side or bottom volumes. |

**Table 12: Variables Defined for Equation (32)**

Q and t were recorded during the tests and $V_1$ was calculated for each level of flow (high, medium, low) using the geometric model in Section 2.8. $V_u$ was a function of porosity and volume of the clay as stated below in Equation 33 below:

$$V_u = SA_1 L_s n_s + A_b L_b n_b + A_L p d n_b \qquad (33)$$

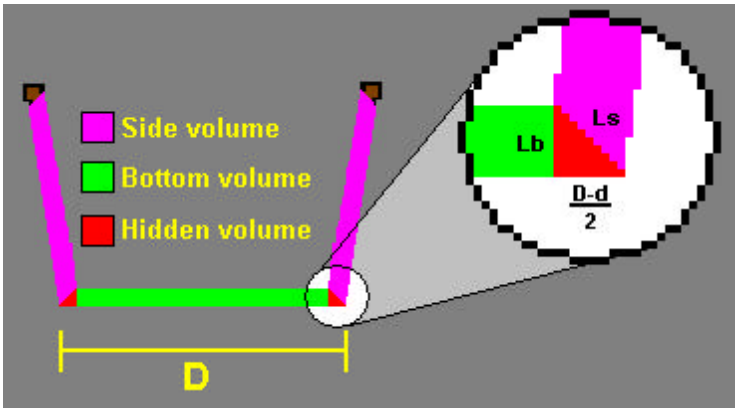


**Figure 17: Filtrón Structural Volume Schematic**

Side and bottom porosity were represented by $n_s$ and $n_b$, respectively. There were two different porosities because I assumed that the bottom of the filter was compressed more during construction therefore it would possibly be less porous then the side ($n_b = n_s$).

The velocity of water, *v'*, which is the average linear velocity, was calculated by using the measured Q divided by the total surface area and weighted porosity. The velocity is not the same as Darcy's velocity in Equations 10 and 11. The equations below illustrate this method:

$$n_T = \frac{n_s SA_1 + n_b A_b}{SA_1 + A_b} \qquad (34)$$

$$v = \frac{Q}{(SA_1 + A_b)n_T} \tag{35}$$

The weighted length, $L_w$, was used to give an overall accurate representation of the average length the water traveled through in the filter.

$$L_w = \frac{L_b A_b + L_s S A_1}{A_b + S A_1} \tag{36}$$

**3.3.2.2 Comparing model to the data**

Each measured data point (conductivity) was compared to a point calculated by the model. Using Excel®, one column was designated as the measured values and the column next to it was the results of the model. Every point had a different U value, increasing because of its dependence on time. The two columns were subtracted from each other (the error) and squared in a third column (the error squared). The total third column was summed into one cell at the bottom of the column (the sum of squared error). If the model followed the data perfectly, the third column (the difference) would equal zero for each point and the bottom sum would equal zero as well.

**3.3.2.3 Using Excel®'s premium solver**

The next step was to solve for the bottom porosity, side porosity, and dispersion coefficient using the Standard Evolutionary solver. This step is similar to finding the hydraulic conductivities as in Phase 1. For the three different levels of flow (high, medium, and low), each of their summed third columns were summed together into one cell for each filter – the cell to be minimized. By finding one set of unknowns (side and bottom porosities and dispersion coefficient) to fit all three levels, the final results would be more consistent with each other provided that the calculated model displayed a similar behavior to the measured data for all three water levels.

First in the solver, I set the total summed cell as the cell to be minimized. The cells to change were the bottom ($n_b$) and side ($n_s$) porosity and dispersion coefficient (D). The following on the next page are the constraints I used:

$n_s$ and $n_b = 0.6$

$n_s$ and $n_b = 0.1$

D = 0.0001 cm/min

$n_b = n_s$

D = 0.2 cm/min

The maximum porosity I assumed was 0.6. Originally, the maximum porosity was set at 0.4 because Nicaragua uses a 40/60 sawdust to clay mixture. If all the sawdust is completely combusted, then the porosity of the Filtrón should be 0.4 assuming that the clay was not porous. In the end, 0.6 was used so that the model could accurately represent the data because the clay could be porous, some small cracks were observed, and this would give the solver more room to

find the answer without artificially constraining the final answer. Anything above 0.6 was too high because the amount of water that would be contained in the filter ceramic was not realistic. If both the bottom and side porosities were 0.6, the maximum amount of water the filter ceramic could contain is about 1300 mL. This maximum value of 1300 mL seems reasonable since I roughly measured the volume of water added to a dry filter, which was about 9 liters. Both the calculated and wet volumetric measurement were around 8 liters, thus making the difference about 1000 mL. The D constraints are very conservative since $D_m$ is equal to 0.0014 cm/min.

After the minimize cell was selected, the changing cells were selected ($n_s$, $n_b$, and D), and the constraints established. Then $n_s$, $n_b$, and D were given and initial guesses of 0.5 for the porosities and 0.2 for the dispersion coefficient. From this point, the solve button was pushed and the changing cells final answers were displayed with the results. Each filter went through this solving process individually.

**3.3.2.4 Calculation of Tortuosity**

With the value obtained for D, the tortuosity (t) could be calculated. The tortuosity was calculated using the following equation defined in the theory section:

$$D = D_m \, t + a_L v \qquad (36)$$

$D_m$ is the molecular diffusion coefficient in water and in this case it is for Bromide. Below is the Wilke-Chang Equation used to calculate $D_m$ (10).

$$D_m = \frac{60 \cdot (5.06 \times 10^{-7}) \cdot (T(Kelvins))}{Am} = 0.0014 \frac{cm}{\min} \qquad (37)$$

$$A = 27 \frac{cm^3}{mol} \text{ for Bromide (atomic volume)}$$

$\mu$ = 0.89 cP @ 25$^o$C (298 Kelvin) (water viscosity)

*T(Kelvins)* = 298 K (average water temperature in the lab)

The longitudinal dispersivity was estimated using the below equation for each filter (15):

$$a_L \text{ (unitless)} = 3.28 \cdot 0.83 \cdot \left[ \log_{10} \left( \frac{L_w}{3.28} \right) \right]^{2.414} \qquad (38)$$

Equation 38 is somewhat uncertain as it was developed for groundwater travel through porous media from a best-fit line to field and experimental data.

The final step is to solve for tortuosity once all the other values in Equation 36 are calculated. The tortuosity was calculated for each filter at each flow level.

$$t = \frac{D - a_L v}{D_m} \tag{39}$$

## Section 4.0 Results

This section presents the results of the research conducted. First, the results and discussion from the Nicaragua trip will be presented, followed by the basic characteristics of each filter tested. Following the basics, the results of the observations that occurred during the laboratory experiments are presented. Concluding this section will be the results from the experimental and numerical methods of the hydraulic conductivity and bromide tracer breakthrough tests. The only two discussions presented in this section are in regards to the trip to Nicaragua and the loading. The remaining discussions will be presented in Section 5.0 Discussion.

### 4.1 Field Results and Discussion

The only results from the trip in Nicaragua that are worth discussing are the microbiological results from the pathogenic indicator organism test performed at Boulder County's Wastewater Treatment Plant by Jon Stoddard (Masters of Science in Environmental Engineering at CU in 2002; former EWB board member). The interviews from the users in San Fransico Libré did not lead to any significant results or conclusions mainly because the wrong set of questions were asked. Alexandra Gabrieloff, the Spanish translator and interviewer on the trip, asked the questions I requested her to use; however, I provided her with the wrong version of the questions. It would have been preferable to use the questionnaire developed and used by Lantagne (See Report 2 – Reference 16) Despite the wrong questions being asked, there was one answer to one question in the last home that she interviewed that will be presented because of its relevance.

At five random homes, water samples of before filtration and after filtration were taken. The afternoon before our departure the samples were put in a cooler with ice to maintain a temperature of about 4 $^{o}$C to reduce the rate of microbiological growth, which would change the pathogen concentrations between the time of sampling and later analysis in Boulder, Colorado. As soon as we arrived at Denver International Airport, I drove directly to the treatment plant in Boulder to deliver the samples to Jon Stoddard who conducted the tests.

It was a Sunday night and not all of the necessary solutions for all of the indicator organism tests were available because they were usually produced Monday morning for routine work in the lab during the week. Jon thought there was enough, but he was mistaken and only one test was performed – Fecal Coliform. The results of the microbiological tests for Fecal Coliform, an indicator organism, at each home's Filtrón are listed on the next page in Table 8. The acronym or unit in the table is MPN or Most Probable Number of the organism.

| Home | Before Filtration (MPN/100mL) | After Filtration (MPN/100mL) | Removal Percentage |
|---|---|---|---|
| 1 | 16000 | <20 | >99.88% |
| 2 | 1700 | <20 | >98.82% |
| 3 | 24000 | 3500 | 85.42% |
| 4 | 230 | <20 | >91.30% |
| 5 | 24000 | 3500 | 85.42% |

**Table 13: San Fransico Libré Field Removal Percentages of Fecal Coliform**

The removal percentage in the table shows that the filters in the field are effective, but not as effective as the filters tested in the labs in previous studies (98 to 100% removal) (7). Homes 3 and 5 are two homes of concern since they had less removal and very high bacterial concentrations. Home 3 according to the interview notes did not mention any health problems while Home 5 did complain. Home 5 complained of diarrhea, cramps, headaches, and dizziness.

These results possibly support Daniele Lantagne's recommendation for education by NGOs about maintenance in her *Report 2: Field Investigations* (16). If the users were maintaining the filters better, maybe the removal rate would be better. There are many possibilities for the different effectiveness of the filters, but since the other homes had descent removal rates, it might be safe to assume that Homes 3 and 5 were not maintaining their filters the same way. Proper education and application of the knowledge gained from the education may have made a difference in Homes 3 and 5. Alternatively, very high loading may have occurred due to poor quality source water, so they may have needed more frequent maintenance.

### 4.2 Basic Filtrón Characteristics

The purpose of this section is to present the measurements and comparison of the calculated volumes and measured volumes. Table 9 summarizes the dimensions of each filter in centimeters (cm) of the conical shape defined in Section 2.8 Basic Filtrón Geometry. The dimension D was not originally defined in the same section; it was defined in Section 3.3.2 Bromide Tracer Breakthrough numerical methods. D is the outer bottom diameter of the filter.

| Filters | 1 | 2 | 3 | 4 | 5 |
|---|---|---|---|---|---|
| Serial # | 18004 | 19499 | 18036 | 17945 | 18193 |
| Units | cm | cm | cm | cm | cm |
| **d** | 18.6 | 18.8 | 18.6 | 18.6 | 19.0 |
| **D** | 20.9 | 21.0 | 20.9 | 20.9 | 21.0 |
| **Ls** | 1.25 | 1.30 | 1.27 | 1.26 | 1.31 |
| **Lb** | 1.50 | 2.00 | 1.50 | 1.40 | 1.60 |
| **h (max)** | 20.3 | 20.4 | 20.4 | 20.3 | 20.3 |
| **r (max)** | 12.8 | 12.9 | 13.1 | 12.9 | 13.0 |
| **s (max)** | 20.9 | 21.1 | 20.9 | 20.9 | 21.1 |

**Table 14: Measurement Summary of the Filters**

Filters 1 and 3 have serial numbers within 40 filters so they might be from the same-fired batch of filters. Filters 2 and 5 have thicker bottoms and sides; they were probably not as compressed as the other filters resulting in more porous filters. Based on the thickness, Filter 4 is the most compressed filter, which possibly is the least porous filter tested. Table 10 summarizes the calculated values from the measurements in Table 9.

| Filters | Units | 1 | 2 | 3 | 4 | 5 |
|---|---|---|---|---|---|---|
| $SA_1$ (max) | $cm^2$ | 1435.06 | 1461.46 | 1460.78 | 1442.22 | 1470.4 |
| $V_1$ (max) | mL | 7776.33 | 7981.6 | 8056.35 | 7851.31 | 8072.3 |
| r (max) | cm | 12.70 | 12.83 | 13.02 | 12.80 | 12.91 |

**Table 15: Calculation Summary of the Filters**

$SA_1$, $V_1$, and r were calculated using Equations 6, 9, and 3 respectively from section 2.8. The geometric model is not perfect as indicated by the differences in radius; however the difference

is less then 1% (within 0.1 cm, which is the measurement precision). Not only was the radius compared to measured values, but also the volumes of Filters 1 through 4 were compared with the calculated value. Table 11 summarizes the calculated versus measured values for volume and radius.

| Filters | $V_1$ (max) mL | | Difference | r (max) cm | | Difference |
|---|---|---|---|---|---|---|
| Origin | Measured | Calculated | % | Measured | Calculated | % |
| **1** | 8140 | 7776 | 4.5 | 12.8 | 12.7 | 0.4 |
| **2** | 8280 | 7982 | 3.6 | 12.9 | 12.8 | 0.5 |
| **3** | 7950 | 8056 | 1.3 | 13.1 | 13.0 | 0.2 |
| **4** | 8210 | 7851 | 4.4 | 12.9 | 12.8 | 0.4 |
| **5** | - | 8072 | - | 13.0 | 12.9 | 0.7 |

**Table 16: Measured Vs. Calculated Values of the Conical Fahlin Model**

The volume difference is less than 5%, which makes it a reasonable model. It is important to note that the volumes were measured once the filters were assumed to be fully saturated with water. It is a possibility that the filters were not fully saturated, which would have left some pores open for water once added. Therefore, the differences might have been less if the filters were not so porous. Measuring the volumes was not an instantaneous process. Water was added by 1 liter increments as fast as possible; however, there would have been ample time for the water to quickly find open pores. This possibility is evident in three out of the four filters measured since the measured value was more than the calculated value. Filter 3 was only 100 mL less than the calculated volume; therefore it could have been fully saturated.

### 4.3 Results and Discussion of the Loading Observations

Figure 16 on the next page is a plot of the simplified Darcy velocity of the water for all the filters, neglecting porosity and the bottom surface area, versus the date:

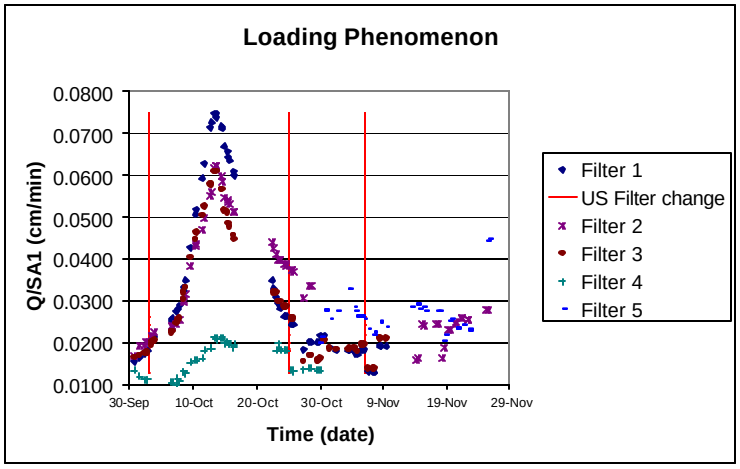


**Figure 18: Filter Loading during Phase One**

All of the filters, except Filter 5, experienced a similar loading phenomenon. One possible reason for the loading is that the source quality of deionized water changed slightly likely

deteriorating over time until the ion exchange resins were changed. The first vertical line in Figure 16 is the date of the first resin change for the deionized water source by United States (US) Filter. During this change, they replaced 2 out of the 4 deionized water resin bottles. During the other changes, they only replaced one of the resin bottle. After the second change, the rate of the velocity slowed down, but it never recovered to the level of the first filter change. One possibility for the increased loading was because there was some biological growth, which was not visible to the eye. The microorganisms grew because the deionized water had more nutrients as the deionized water filters were being exhausted and more water traveled through the Filtróns.

No analysis of the microorganisms on the surface of the filter was attempted. One possibility of growth could have been algae since the Filtróns were not covered and were subject to 24 hours of fluorescent light every day. By the end of the October, the surface on the filters felt smoother to the touch than when the testing began. This observation indicates the possibility of biological growth. In addition, the short clear plastic tubing, not shown in Figure 13, after the ball valve that led to the sink had some type of light brown growth in the path of the water.

Because of the loading phenomena, a total organic carbon (TOC) measurement was conducted to try and improve our understanding. Each filter (with colloidal silver) was measured after filtration and the deionized source water was measured. Below are the results of the measurement:

| Filters | Deionized Water | 1 | 2 | 3 | 4 |
|---|---|---|---|---|---|
| TOC (ppb) | 96±4 | 362±24 | 416±8 | 180±2 | 197±1 |

**Table 17: Total Organic Carbon Test**

The results of the measurement show an increase in TOC. Something was adding carbon to the water and two possibilities come to mind – (1) biological activity and (2) carbon from the sawdust. Biological growth could be contributing to the carbon from their waste. This includes extracellular polymeric substrates (EPS). If heterotrophs such as bacteria were the culprit, the results of the TOC test would violate the carbon mass balance so the biological activity was likely dominated by autotrophs such as algae. Autotrophs fix, or collect, carbon dioxide from the atmosphere for their growth, and most algae are known to release organics into the water. Carbon could also come from the sawdust that was not completely combusted or any charcoal that was left inside of the Filtrón. This possibility seems unlikely since the filters were fired at a high temperature over long time periods during construction and there was more than enough time for the carbon to wash out during the nitrate study and the research conducted before the TOC measurement was taken. More research testing of TOC across the filter is needed in the future.

Testing directly for the biological growth would have answered the question about biological activity; however, I did not have the laboratory skills or facilities available to directly test for the biological growth. I was not expecting to test the loading rate of the filters and their causes. Milli-Q® water should have been used and the filters should have been in a dark room or covered to alleviate the possibility of biological growth. Before I started this research, I assumed that the colloidal silver would inhibit the possibility of biological growth and it probably did for a while until enough nutrients and energy from the light were available to allow some growth and cause

loading to reduce the flow as well as the possibility that the silver concentration depleted over time.

Another twist to the possibility of the loading phenomena could be that the deionized water quality was not a considerable factor at all. The reason for the loading could be that the silver is no longer affective once all the colloidal silver contact sites with the water were overcome with microscopic substances such as organic carbon from either the filter itself or the water. This would allow biological growth to occur at an increased rate clogging the filter and reducing the velocity of the water through the filter. Instead of or in combination with the colloidal silver contact sites being overcome with microscopic substances, the silver could slowly "strip" out of the filter over time and use.

The "stripping" concept is supported by Daniele Lantagne's results concerning the concentration of silver in consecutive runs. In Lantagne's report, 5 mL of 3.2% solution was added to a filter that was tested for the final silver concentration in the treated water in micro-grams per liter (µg/L) on three consecutive runs. 37, 17, and 14 µg/L were the consecutive run effluent silver concentrations (3). Her results show that the filter does "strip" silver over initial use, but the long term "stripping" is a question still that needs to be answered, especially in this case. Over a year's time if the amount of silver stripped after each run remained constant at 14 µg/L, the filter would have almost six times the amount of silver needed for a year's use according to the mass balance in Appendix C. It would be interesting to know the stripping involved if the filters were exposed to different levels of loading during field home use.

### 4.4 Hydraulic Conductivity Test Results

The numerical methods described in Section 3.3.1 that produced the results are somewhat confusing. Figure 17 on the next page will help summarize the methods so that the results will be less confusing.

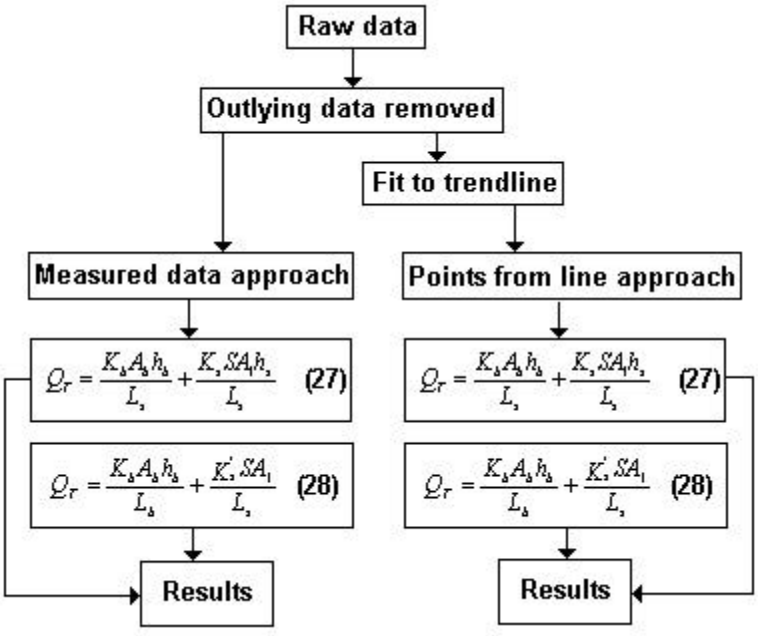


**Figure 19: Flowchart Summary for Hydraulic Conductivities Numerical Methods**

The flowchart shows that there are two sets of results from the two approaches – measured data, or data for short, and points from line, or line for short. Within each approach are two sets of results from the different equations used making a total of four separate results for each filter. Table 13 summarizes the four sets of results for each filter in m/hr instead of cm/min so that they could be compared to the results from the Eriksen Model.

| | Equation 27 | | | | | | Equation 28 | | | |
|---|---|---|---|---|---|---|---|---|---|---|
| **Approach** | **Data** | | | **Line** | | | **Data** | | **Line** | |
| **K** | **$K_b$** | **$K_s$** | **F** | **$K_b$** | **$K_s$** | **F** | **$K_b$** | **$K'_s$** | **$K_b$** | **$K'_s$** |
| Units | m/hr | m/hr | - | m/hr | m/hr | - | m/hr | $m^2$/hr | m/hr | $m^2$/hr |
| **1** | 0.000863 | 0.007460 | 0.080 | 0.001028 | 0.054541 | 0.011 | 0.000006 | 0.000134 | 0.000006 | 0.000136 |
| **2** | 0.001316 | 0.001847 | 0.509 | 0.001607 | 0.004948 | 0.185 | 0.000006 | 0.000191 | 0.000006 | 0.000191 |
| **3** | 0.001184 | 0.005107 | 0.114 | 0.001263 | 0.010784 | 0.056 | 0.000006 | 0.000137 | 0.000006 | 0.000142 |
| **4** | 0.000006 | 0.007417 | 0.072 | 0.000006 | 0.015223 | 0.035 | 0.000006 | 0.000081 | 0.000006 | 0.000079 |
| **5** | 0.001036 | 0.002874 | 0.371 | 0.000006 | 0.020869 | 0.334 | 0.000006 | 0.000204 | 0.000006 | 0.000209 |

**Table 18: Hydraulic Conductivity Results**

For Equation 27, $K_b$ is less than $K_s$ as assumed and restrained by the solver. Excluding Filter 4, Kb ranges from 11 to 71% of the $K_s$ for Equation 27 Data. The same trend is true for the Line results with the exception of Filter 5, which is not close to the Data result. For Equation 28, all of the results for $K_b$ were the minimum value of 0.000006 m/hr. The corresponding values of $K_s$ for the Data and Line approaches were very close to each other.

Both of the equations were used with the results in Table 13 to try and model the flow for the Bromide Tracer Breakthrough Test. Neither of the equations accurately modeled the flow for the tracer test so their accuracy is in question, which will be further analyzed in the discussion section.

### 4.5 Bromide Tracer Breakthrough Tests Results

The results from the tracer tests are broken into two sections – breakthrough times and tortuosity factors. The determination of the breakthrough times was not discussed in the methods section, but it will be discussed in the next section and their relevance. The tortuosity factors section will not only present the tortuosity factors calculated, but it will also present the basic values needed to calculate the tortuosity. The basic values are the porosities and dispersion coefficient results from the Standard Evolutionary solver.

#### 4.5.1 Breakthrough Times

Two breakthrough times were estimated by interpreting the plot from the measurements. The initial breakthrough time was the first time that Bromide exceeded background levels as determined directly using the plotted data. The first data point represented it where the electrical conductivity increased significantly after the delay time. Figure 18 is a representation of this method performed on Filter 5 for the high flow rate test.

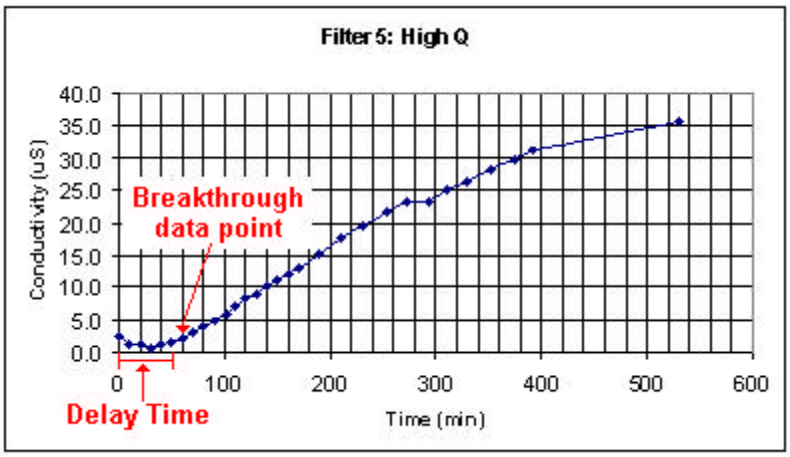


**Figure 20: Initial Breakthrough Time for Filter 5 High Flow Rate**

The breakthrough time may not be the most obvious point. In this case, the data was directly investigated showing a large conductivity value change (=0.2 µS = detectable electrical conductivity change) between the 50$^{th}$ and 60$^{th}$ minute of the test for the high flow rate test for Filter 5 (60 minutes). The delay time in the figure is 50 minutes.

The second breakthrough time is the 50% conductivity breakthrough time. This was the time that the filter effluent reached 50% of the spiked source conductivity. A similar method to initial breakthrough time was used for this time determination; a plot was used. For this time determination, a 50% conductivity horizontal line was plotted on the same plot as the corrected electrical conductivity data from the experiment. Data was corrected for baseline conductivity since the actual measurements never resulted in zero µS in the beginning, thus the baseline conductivity was subtracted from the actual measurement. The time in which the data curve and the 50% conductivity line intersect is the 50% conductivity breakthrough time. Figure 19 is a representation of this method performed on Filter 5 for the high flow rate test.

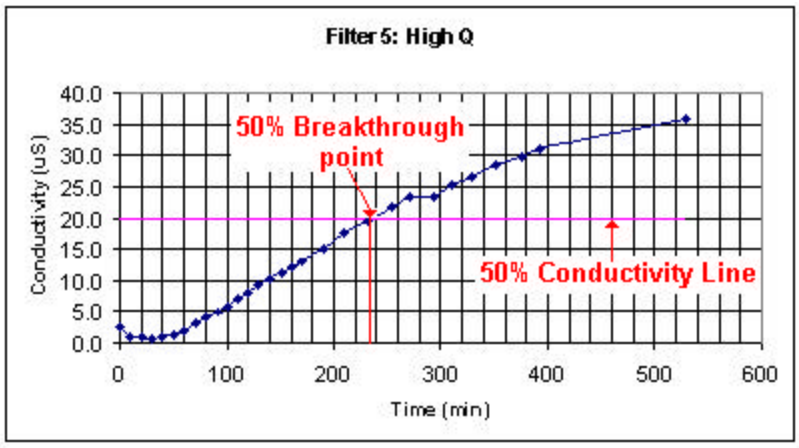


**Figure 21: 50% Conductivity Breakthrough Time for Filter 5 High Flow Rate**

To accurately determine the intersection point, the plot was zoomed in using Excel® to get a better picture of the intersection. The 50% conductivity breakthrough time for this example was 236 minutes.

The relevance of these times might be the most important numbers for Potters for Peace. The initial breakthrough time is the minimum amount of time the water was in contact with the wall of the filter and the 50% conductivity breakthrough time is the average amount of time the water was in contact with the wall of the filter. These times should not be confused with the time in the pores. The times are not the minimum and average time inside the pores of the filter; they are the times one molecule of water from the moment in drops into the filter to the time it exits the receptacle.

An important note is that the delay water volume at the bottom of the receptacle for all the filters including the blank was full with "improved" deionized water once the tracer was spiked into the inflow. As the bromide tracer water dripped into the delay volume of the blank, the initial breakthrough of the delay volume occurred within 10 minutes of the experiment resulting in no significant delay time for the tracer. Thus, the times determined from the graphs were not adjusted for any delay time since it was negligible (<10 minutes).

Furthermore, the time the tracer was in the initial volume of the water inside the Filtrón before passing through the wall was estimated using the hypothetical detection time method. Due to dilution of the bromide into the "improved" deionized water in the Filtrón, it would not be immediately measurable using the sensitivity of the conductivity probe. This time was also found to be negligible since it was less than two minutes. See Appendix D for the calculation of this estimate. Table 14 on the next page summarizes the results of the breakthrough time results.

| | | Q | Volume | Initial Breakthrough Time | Volume % | 50% Conductivity Time | Volume % |
|---|---|---|---|---|---|---|---|
| | Units | mL/min | mL | min | % | min | % |
| #1 | **High** | 32.3 | 8409 | 60 | 23.02% | 268 | 102.84% |
| | **Medium** | 19.1 | 8009 | 140 | 33.39% | 429 | 102.31% |
| | **Low** | 14.6 | 7717 | 152 | 28.84% | 515 | 97.70% |
| #2 | **High** | 45.6 | 8622 | 50 | 26.44% | 210 | 111.06% |
| | **Medium** | 20.9 | 6596 | 91 | 28.88% | 365 | 115.84% |
| | **Low** | 14.9 | 6342 | 116 | 27.19% | 397 | 93.14% |
| #3 | **High** | 35.3 | 8375 | 60 | 25.31% | 239 | 100.83% |
| | **Medium** | 21.0 | 8172 | 90 | 23.13% | 391 | 100.48% |
| | **Low** | 16.1 | 7729 | 152 | 31.62% | 480 | 99.86% |
| #4 | **High** | 23.2 | 8629 | 110 | 29.58% | 373 | 100.29% |
| | **Medium** | 10.6 | 8301 | 297 | 37.78% | 831 | 105.72% |
| | **Low** | 5.6 | 8301 | 362 | 24.42% | 1298 | 87.55% |
| #5 | **High** | 33.7 | 7765 | 60 | 26.07% | 236 | 102.53% |
| | **Medium** | 20.0 | 5384 | 60 | 22.29% | 276 | 102.53% |
| | **Low** | 13.5 | 5036 | 116 | 31.17% | 404 | 108.57% |

**Table 19: Breakthrough Time Summary**

The volume in the table is

$$V_1 + \text{delay volume} = Volume \qquad (40)$$

The volume percentage is

$$\frac{Qt}{Volume} = Volume\,\% \qquad (41)$$

where t is the either the initial breakthrough time or the 50% conductivity time.

### 4.5.2 Tortuosity Factors

The tortuosity factors where solved for once the side porosity, bottom porosity and dispersion coefficient were determined using the Standard Evolutionary solver. The primary focus of the solver was to accurately resemble the data with the simplified model discussed in the numerical methods section. On the next page are the plotted results of measured and calculated values for all three runs for Filter 3. All of the tracer results for every filter for every run are given in Appendix E.

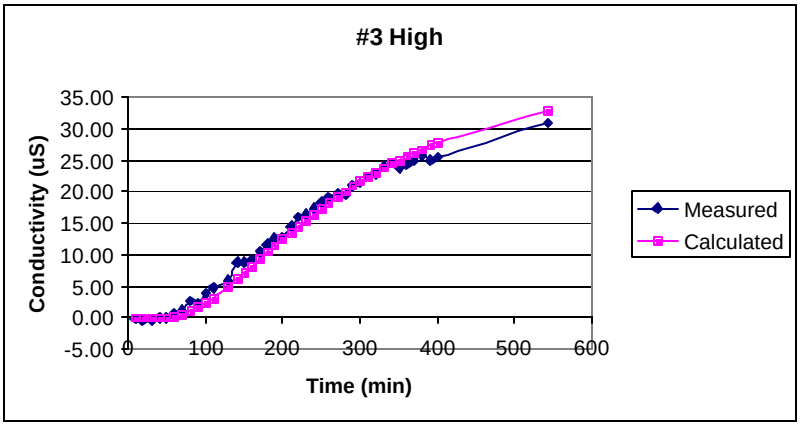


**Figure 22: High Flow Filter 3 Bromide Tracer Plot**

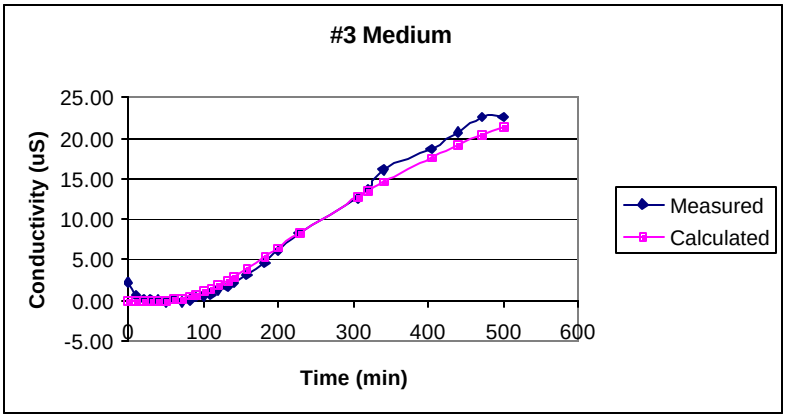


**Figure 23: Medium Flow Filter 3 Bromide Tracer Plot**

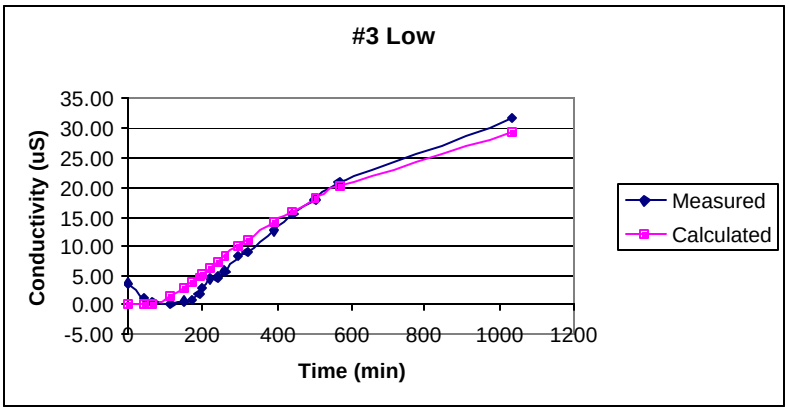


**Figure 24: Low Flow Filter 3 Bromide Tracer Plot**

Figures 20 through 22 show good agreement between the measured conductivity breakthrough and the modeled curves (calculated curves).

The summary of the solver results are in Table 15 for the porosities and dispersion coefficient.

| | | Side Porosity | Bottom Porosity | Overall Porosity (Weighted) | $V_u$ | Dispersion Coefficient |
|---|---|---|---|---|---|---|
| **Filters** | **Units** | **ns** | **nb** | **nt** | **mL** | **$cm^2$/min** |
| #1 | **High** | 0.6000 | 0.6000 | 0.6000 | 1296.94 | 0.007605 |
| | **Medium** | 0.6000 | 0.6000 | 0.6000 | 1248.41 | 0.007605 |
| | **Low** | 0.6000 | 0.6000 | 0.6000 | 1212.67 | 0.007605 |
| #2 | **High** | 0.6000 | 0.6000 | 0.6000 | 1452.56 | 0.012971 |
| | **Medium** | 0.6000 | 0.6000 | 0.6000 | 1194.36 | 0.012971 |
| | **Low** | 0.6000 | 0.6000 | 0.6000 | 1160.92 | 0.012971 |
| #3 | **High** | 0.6000 | 0.1552 | 0.5251 | 1093.92 | 0.011628 |
| | **Medium** | 0.6000 | 0.1552 | 0.5236 | 1069.33 | 0.011628 |
| | **Low** | 0.6000 | 0.1552 | 0.5200 | 1015.37 | 0.011628 |
| #4 | **High** | 0.1544 | 0.1000 | 0.1455 | 314.44 | 0.017700 |
| | **Medium** | 0.1544 | 0.1000 | 0.1452 | 304.23 | 0.017700 |
| | **Low** | 0.1544 | 0.1000 | 0.1452 | 304.23 | 0.017700 |
| #5 | **High** | 0.2407 | 0.1000 | 0.2145 | 442.81 | 0.032771 |
| | **Medium** | 0.2407 | 0.1000 | 0.2053 | 316.54 | 0.032771 |
| | **Low** | 0.2407 | 0.1000 | 0.2032 | 297.28 | 0.032771 |

**Table 20: Porosity and Dispersion Coefficient Summary**

All of the filters were affected by the constraints since all of the filters either had a side porosity of 0.6 or bottom porosity of 0.1, which were the constraints put into the solver. Only 3 of the filters (Filters 3 – 5) had bottom porosities less than side porosities. The other two filters had side and bottom porosities equal to each other. In addition, the dispersion coefficients ranged from about 0.01 $cm^2$/min to 0.03 $cm^2$/min. Furthermore, the unknown volume, Vu, the volume of water inside the walls of the filter in the pores, ranged from as high as 1300 mL to as low as 300 mL.

Using the results in Table 15, the tortuosity was calculated using Equations 37 through 39. The results of the calculations are given in Table 16.

| | | Dispersion Coefficient (D) | Long. Dispersivity ($a_L$) | Molecular Diffusion ($Br^-$) ($D_m$) | Tortuosity Factor (t) | |
|---|---|---|---|---|---|---|
| **Filters** | **Units** | $cm^2/min$ | cm | $cm^2/min$ | - | **Average** |
| #1 | **High** | 0.007605 | 0.0780 | 0.0014 | 3.6 | 4 |
| | **Medium** | 0.007605 | 0.0782 | 0.0014 | 4.3 | |
| | **Low** | 0.007605 | 0.0783 | 0.0014 | 4.5 | |
| #2 | **High** | 0.012971 | 0.0912 | 0.0014 | 6.3 | 7 |
| | **Medium** | 0.012971 | 0.0942 | 0.0014 | 7.5 | |
| | **Low** | 0.012971 | 0.0948 | 0.0014 | 7.9 | |
| #3 | **High** | 0.011628 | 0.0796 | 0.0014 | 5.9 | 7 |
| | **Medium** | 0.011628 | 0.0797 | 0.0014 | 6.8 | |
| | **Low** | 0.011628 | 0.0799 | 0.0014 | 7.1 | |
| #4 | **High** | 0.017700 | 0.0773 | 0.0014 | 7.3 | 10 |
| | **Medium** | 0.017700 | 0.0774 | 0.0014 | 10.1 | |
| | **Low** | 0.017700 | 0.0774 | 0.0014 | 11.3 | |
| #5 | **High** | 0.032771 | 0.0858 | 0.0014 | 17.0 | 18 |
| | **Medium** | 0.032771 | 0.0878 | 0.0014 | 17.9 | |
| | **Low** | 0.032771 | 0.0882 | 0.0014 | 19.4 | |

**Table 21: Tortuosity Results**

Results of from the model showed that tortuosity factors ranged from 4 to 19 and were generally similar for the three flow rates with the same filter.

## Section 5.0 Discussion

### 5.1 Hydraulic Conductivity Test Discussion

As mentioned in the results section, the accuracy of the results is in question. For this discussion, the results from Equation 27 will present first followed by the discussion about Equation 28. Concluding this section of discussion will be the comparison between the two equations, Eriksen Model results, and Lantagne's updates.

#### 5.1.1 Equation 27

For this section, the results from the data approach will be discussed first followed by the line approach.

$$Q_T = \frac{K_b A_b h_b}{L_s} + \frac{K_s S A_1 h_s}{L_s} \qquad (27)$$

Equation 27 used Equation 26 for the side head ($h_s = F h_b$). Filters 1, 3, and 4 had F factors less then 0.12 with large $K_s$, which do not seem reasonable. According to this logic, on average, only 2.4 cm of head at 20 cm of vertical water inside the filter ($h_b$) would drive the water through the side. Since F and Ks are multiplied to together and solved for using the solver, F could be larger while $K_s$ could be smaller resulting in a similar answer as before.

Filters 2 and 5 have results that seem explainable and logical versus the results from the other filters. Both of the filters had reasonable F factors with similar side and bottom conductivities between the two. The lowest F factor was 0.37 and according to that logic, the head driving the water through the side for 20 cm was averaged at 7.4 cm. This result seems logical that the

average head is not less than 2 cm to drive the water through the side. One would predict an F value near or less than 0.5 to represent the "average" but this F should be weighted since more flow area is present at the larger "top" when less head is available.

The results from the line data did not represent the same trends as the data approach as expected; therefore giving more support for the questionable accuracy of this method by using the F factor. Filter 5 was the only filter that had a similar trend i.e. that the F factor was close to the data approach; however, the hydraulic conductivities differed.

The only results that seemed reasonable for using Equation 27 for modeling the water flow through the filter is the data approach for Filters 2 and 5. Two approaches (data and line) were used and both had different results with no similar trends between the two approaches except one. Thus, there is no certainty to the results using Equation 27 in the fashion that was performed using the F factor.

The solver if given the proper constraints such as accurately modeling the side head would likely produce consistent data for the results in future research with reasonable certainty. Results could likely be improved by more grouping data points into a single solver run and without potential loading causing the water height behavior of the filter to change over time.

### 5.1.2 Equation 28

For this section, the results from the data and line approach will be discussed to at the same time.

$$Q_T = \frac{K_b A_b h_b}{L_b} + \frac{K_s' S A_1}{L_s} \qquad (28)$$

According to the results using Equation 28, very little if any water travels through the bottom of the filters. Every single $K_b$ for both approaches had the same $K_b$ equal to 0.000006 m/hr, which is the minimum number put into the solver (0.00001 cm/min = 0.000006 m/hr). The minimum number was established so that $K_b$ could not equal zero. By having the $K_b$ essentially equal zero, this model does not seemed reasonable for modeling the flow although both approaches had the same trends and similar results.

Equation 28 fit the selected points well; however, using Equation 28 as a model of flow is not the best method since virtually none of the water flows through the bottom. This violates Lantagne's 17% water flow through the bottom result by painting the sides of the filter (3). Granted, the filters she used are different filters and the filters used in this experiment may have had plugged bottom pores since there was some biological growth; however, it seems illogical that no water went through the bottom given the wide range of head that was in the filter during the testing, especially in the beginning when there was no time for growth.

### 5.1.3 Comparisons between Equation 27 and 28, Eriksen's Model, and Lantagne's Update

Equation 27 or 28 did not have similar results as expected since they were different models; however, I did not expect that they would be completely different. If the bottom pores were plugged, I would think that Equation 27 would reflect the same results for $K_b$ as did Equation 28; but they did not. Neither equation is accurate enough to represent the flow. The only results

worth mentioning for the future comparison are Filters 2 and 5 using Equation 27 method with the data approach.

Both equations were used to try and model the flow rate for the Bromide Tracer Breakthrough Tests so that they could be compared to the actual flow. Neither Equation 27 nor 28 accurately modeled the flow for the tracer test; they were off on average by more than 5 mL/min (30%).

The problem for both modeling equations could lie in the fact that the relationship between the flow and the surface area is not linear as assumed earlier. Recalling from the methods section, the method in which the data was selected for the points used in the solver were determined by eliminating nonlinear or outlying data. This may not be the best method. The linear relationship is unlikely to be linear since the accurate model, which still has to be determined, for side head may not be linear or the side hydraulic conductivity, $K_s$, varies at different side depths. I strongly recommend future research to head in this direction – modeling the side head.

The only reasonable results from Filter 2 and 5 are presented in the Table 17 with Eriksen's results and Lantagne's update of his model.

| | Eriksen | Lantagne | Equation 27: Filter 2 | | Equation 27: Filter 5 | |
|---|---|---|---|---|---|---|
| | $k_{actual}$ | $k_{actual}$ | $K_b$ | $K_s$ | $K_b$ | $K_s$ |
| Units | m/hr | m/hr | m/hr | m/hr | m/hr | m/hr |
| **Value** | 0.03 | 0.004 | 0.001316 | 0.001847 | 0.001036 | 0.002874 |

**Table 22: Hydraulic Conductivty Comparison**

Assuming that the values from Filter 2 and 5 are accurate, the flow through the filter is slower than the Eriksen model predicted even when Lantagne improved his assumptions.

### 5.2 Bromide Tracer Breakthrough Tests Discussion

This section will discuss the results presented in the earlier section with the addition of the one more result not presented earlier – the estimated length of the colloidal silver layer. First, both types of breakthrough times will be discussed followed by the tortuosity factors.

#### 5.2.1 Breakthrough Times

According to the results, the water remains in the filter for a considerable amount of time. The earliest the bromide tracer could be detected in the initial breakthrough time was 50 minutes at the high flow rate. Again, the initial breakthrough time is not the $T_{min}$ (time minimum for colloidal silver contact) in the Eriksen Model. It is the minimum amount of time the tracer could be detected coming out of the receptacle; however since the time in the filter and the time in the delay volume was considered negligible, it is likely to be a good estimate of the minimum amount of time the water is in the pores of the filter.

Assuming the initial breakthrough time is as good estimate for time in the pores, there should be plenty of time for contact with the silver depending on the thickness of the silver layer. If the silver completely lined the internal pore surface of the filter from the inside to the outside, 50 minutes at a lower concentration of silver currently used by Potters for Peace should be adequate for inactivation. This is assuming that the 25 minute minimum contact time used by Eriksen and

the 20 minute contact time from Microdyn (the manufacturer of the colloidal silver) has any merit with regard to a desirable inactivation (such as 99.9%).

All the discussion so far has been about the minimum amount of time the water would have contact with the silver from the initial breakthrough time, but the average time needs to be mentioned. The minimum average time for the largest flow rate from the 50% conductivity tests was 210 minutes with a maximum time of 268 minutes excluding Filter 4 since it was operating slower than 1 L/hr at the end of the tracer tests. These results indicate that there is ample time for contact with the majority of the water. However, good contact time for inactivation information is needed to confirm that sufficient pathogen inactivation could occur.

### 5.2.2 Tortuosity Factors

The tortuosity factors that were determined ranged from 3.6 to as high as 19.4 for the non-colloidal silver filter – Filter 5. Filters 2 and 3 had similar tortuosity factors while the other filter's tortuosity factors varied considerably from each other, but there was one consistent trend in each succession of the flow rate level (high, medium, low).

The main trend was that as the weighted length ($L_w$) increased at each flow level, the tortuosity factor increased as well. This may possibly explain the wicking phenomenon that was observed. As the water level decreased inside the filter as a result of the decreasing flow, the water would take a more tortuous path i.e. traveling a greater distance up the filter from the capillary action.

### 5.2.3 Estimated Length of the Colloidal Silver Layer

This subsection will discuss the estimated colloidal silver layer because these results are a consequence of the porosities determined in Section 5.2.2 Tortuosity Factors. The resulting porosities varied considerably; therefore, the thickness of the colloidal silver layer will also vary. Filters 1 and 2 maximized the constraints for solver with bottom porosities equally 0.6 with a pore volume ($V_U$) equal to 1297 mL. Filter 3 maximized the side porosity, but did not for the bottom porosity. Filters 4 and 5 maximized the bottom porosity but not the side porosity. Either this variation is a result of an error within the mathematical methods or an indication that the filters are not uniform with many cracks that greatly influence the porosity. Ideally, it would be more accurate if we knew the overall porosity through experimental methods at each level of water within the filter. This way the solver could focus on one unknown (dispersion coefficient – D) versus three ($n_b$, $n_s$, and D). Otherwise, both porosities could be set to 0.4 since 0.4 is the hypothetical porosity due to the 40/60 sawdust to clay mixture in construction and then the solver could focus only on the dispersion coefficient.

Assuming the results are accurate, the colloidal silver layer was calculated by

$$\frac{252mL}{V_U} L_w = \text{colloidal silver layer (c)} \qquad (42)$$

The factor that is multiplied by $L_w$ is the ratio between the volume of the solution added by PFP and the volume of the pores. Table 18 summarizes the results from this calculation for the highest flow rate on the next page.

| Filter | Colloidal Silver Layer (c) |
|---|---|
| Units | mm |
| **1** | 2.5 |
| **2** | 2.5 |
| **3** | 3.0 |
| **4** | 10.0 |
| **5** | 8.0 |

**Table 23: Colloidal Silver Layer Thickness Estimation**

All of the estimates are above Lantagne's 2 mm estimation; however her estimate is still a good conservative approximation.

### 5.3 Final Comparison between Eriksen, Lantagne, and Fahlin Results

This subsection is devoted to comparing the theoretical hydraulic conductivites ($k_{max}$). This will be accomplished by assuming the initial Eriksen model is valid and my tortuosity and measurement results will be used to compare the values with Eriksen's initial guess and Lantagne's corrected update.

To recall, Equation 25 in Section 2.9.4 was used to calculate the maximum hydraulic conductivity of the filter as

$$k_{\max} = \frac{cb}{T_{\min} H} \qquad (25)$$

Eriksen derived it and Lantagne used Equation 25 to calculate her values. The same $T_{min}$ will be used for my calculation of $k_{max}$ assuming the 25 minute minimum contact time for the colloidal silver is valid; however, all of the other values will differ. Equation 25 is modified for the comparison by displaying tortuosity (t) in Equation (43).

$$k_{\max} = \frac{ctb}{T_{\min} H} \qquad (43)$$

Table 19 summarizes the parameters used in Equation (43) and the resulting $k_{max}$ values, which are highlighted in green. Parameters $H$ and $b$ are h and $L_b$ in the Fahlin model.

| Parameter | Units | Eriksen | Lantagne | Fahlin | |
|---|---|---|---|---|---|
| ***c*** | m | 0.0001 | 0.0020 | 0.0025 | 0.0100 |
| **t** | - | 1 | 2 | 4 | 19 |
| ***b*** | m | 0.010 | 0.010 | 0.0145 | 0.0145 |
| $T_{min}$ | min | 25 | 25 | 25 | 25 |
| ***H*** | m | 0.24 | 0.24 | 0.2034 | 0.2034 |
| $k_{max}$ | m/hr | 0.00001 | 0.00040 | 0.00171 | 0.00325 |

**Table 24: Maximum Hydraulic Conductivity Comparison**

Recall in Section 5.1.3 in Table 17 that the actual (questionable) hydraulic conductivities (both bottom and side) for Filters 2 and 5 ranged from 0.00104 to 0.00287 m/hr. Furthermore, the

overall actual hydraulic conductivity of Eriksen's and Lantagne's work were 0.03 and 0.004, respectively.

Even though the Fahlin Model is fundamentally different by geometry, the Eriksen Model for the maximum hydraulic conductivity (Equation 25) is close to this research's experimental results (when using updated values). However, more research is needed to improve this concept, especially since the results from the research with regard to actual hydraulic conductivities is questionable.

## Section 6.0 Recommendations

This section is devoted to the recommendations for Potters For Peace and future researchers. Unfortunately for Potters For Peace, I only have one immediate recommendation; however, I have many recommendations for future research. Hopefully, results from future research will clear-up many uncertainties contained in this research and give Potters For Peace something tangible and more useful in the future.

### 6.1 Potters for Peace Recommendations

The only recommendation for Potters For Peace is to try new methods of colloidal silver application to fully utilize the entire path of water flow through the filter for contact with inactivating silver. I understand that Ron Rivera, who has been working on the development of the filter for over a decade now, has probably tried many different methods. My recommendation is not to increase the cost or increase the complexity of the colloidal silver application. My recommendation is to try and develop a way that colloidal silver can be added so that the entire pore structure, internal and external, is lined with an effective concentration of silver.

Currently, the pore structure is not fully lined by colloidal silver as indicated by the results from this research and assumed by previous studies. In addition, results from the field show that the filters have been decreasing their rate of filtration between the $6^{th}$ and $14^{th}$ month of use, which could be a result of many different possibilities (17). Since the pores are not fully impregnated with silver, one likely possibility is the internal pores not lined with silver become clogged with biological growth not susceptible to cleaning procedure of the outer surface as recommended by Potters For Peace.

My recommendation could be accomplished by Potters For Peace doing it onsite with local materials and in cooperation with another organization similar to Alethia Environmental using materials found in Nicaragua. The cooperating organization could take non-impregnated with silver filters from the Nicaragua workshop and test different application methods with varying concentrations of the colloidal silver to optimize the method for easy application with maximum removal while keeping the cost to a minimum.

The method I recommend trying is submerging each filter in a container filled with the colloidal silver solution at different concentrations and for varying time intervals. After the filter has been given this "colloidal silver bath," it would then drip into a non-reactive bucket for collection of the excess silver solution. After it stopped dripping, the excess solution could be recycled, thus

reducing the amount of wasted solution. Next the filter would be allowed to dry and be tested in the laboratory for biological removal and silver concentration over a determined time of use.

The possible outcome from optimizing the colloidal silver application could be extending the time of use or life of the filter by reducing the internal biological clogging while maintaining a high removal percentage.

It must be noted that by increasing the time of contact with silver by adding more silver or adding silver to all of the pore length does not imply changing the construction of the filter for an increased flow rate. Until more information is know about silver inactivation and the accurate pore size of other filters using different mixes of clay, the current construction mix should not be altered even though it is tempting. It is tempting since the slow flow rate is usually a complaint from users (16).

### 6.2 Research Recommendations

This subsection is divided into two elements of research – (1) immediate research recommendations directly related to this investigation and (2) separate research.

#### 6.2.1 Directly Related Immediate Research Recommendations

In this research, there were three areas that could be improved to get better and/or more accurate results and my recommendations concern these areas. The first area is Phase One – the hydraulic conductivity tests. The second area is related to Phase One but is focused on the side head modeling and lastly the third area is measurements of the volumetric porosity.

My first recommendation is to repeat Phase One with slightly different methods. Since autotrophic, or algae, microorganisms seemed to be the biological growth the caused some clogging, I suggest reducing the amount of measurements, minimizing light exposure, and using Milli-Q® water versus deionized water. I took many measurements over a 40-day period for most of the filters at many different and random times. I originally thought that the filter would have the same measurements at the same flow rate regardless of the sequence of time (the date). I was wrong because there were days when the height of the water differed by more than 5 cm at the same flow rate as a previous day. As a result, I recommended starting at 40 mL/min and end with 5mL/min by decreasing the flow rate by 5 mL/min per day while taking three measurements per day at the same flow rate. This would take 8 days and then for curiosity's sake start at 5 mL/min and increase by 5 mL/min until 40 mL/min is reached. During the test, the filters would be covered to minimize the amount of light and MQ water would be used. Milli-Q® water would be used to minimize the amount of substrate or carbon for microorganisms to use.

Ideally, this recommendation would reduce the possibility of clogging. Furthermore, this recommendation would likely eliminate outlying or insignificant data; therefore, all the data could be used. It must be noted that the data will more likely not be linear like I assumed, which brings me to my second recommendation – side head modeling.

The biggest drawback to this research is the modeling of the side head to be used in Darcy's Equation. To recall, neither Equation 27 nor 28 accurately represented the flow in Phase Two –

Bromide Tracer Breakthrough Tests. I assumed it was linear and it may be at points; however it does not accurately represent the flow at all levels of flow in the filter. Consequently, the side head may not have a linear relationship as assumed. Therefore, I recommend investigations into modeling the side head so that the proper mathematical model can be used to accurately represent the data. The wicking phenomenon may make the side head modeling complicated. Ideally, if the side head is accurately modeled with the same measurements of h, S, and Q, it may be possible to use my data to compare it to new research.

My third and final recommendation for directly related immediate research is to measure the volumetric porosity of all the filters used in this research so that the accurate overall porosity could be used instead of solving for it as I did. This would enable the solver to only find one unknown – the dispersion coefficient (D). One method I recommend is using a known volume of water in a container that the filter can fit in completely. A completely dry filter would be submerged in the water for an extended period of time (more than four hours). Eight hours is recommended since the filters are submerged overnight before their flow rates are tested in Nicaragua. Once the filter has become saturated with water, the filter should be lifted out of the water and the water contained inside the filter (not the pores) should be emptied into the container quickly to minimize the loss of water due to filtration. The next step would be to let the filter drip the excess water into the container for no more than two minutes. Measure the amount left in the container and subtract the beginning volume from the final volume. The difference between the two measurements will be the overall porosity.

At least three different measurements of the overall porosity at different water level heights in the filter should be conducted. Starting with the complete submergence followed by half submerged then one quarter submerged. In addition, if the researcher wants to use my raw data they should test for the porosity at the same level of water for each filter for each test. Before submergence, the filter should be completely dry. To speed-up the process between tests, the filters could be "baked" in an oven to vaporize any water trapped in the pores.

An alternative method for finding the overall porosity could be by measuring the change in water level after the filter is submerged in a container of a known volume of water.

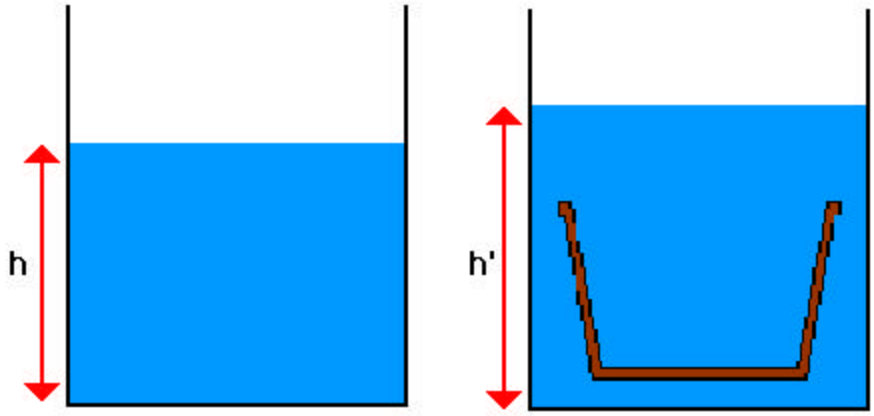


**Figure 25: Porosity Measurement by Height of Water Test**

To find the porosity, we would need the volume of water before submergence (V), the volume of the water after submergence (V'), the geometric volume of the filter with the pore ($V_{geometric}$). V could be found by multiplying the cross-sectional area times the height (h). V' would be calculated the same way but with h' instead of h. The difference between V and V' is the volume of the solids ($V_{solids}$). The total volume of the pores ($V_{pores}$) is equal to the difference between $V_{geometric}$ and $V_{solids}$. Finally, the porosity is equal to $V_{pores}$ divided by $V_{solids}$. It must be noted that the filter must be completely dry before submergence and the filter should be allowed to soak for longer than 2 hours to ensure complete saturation of the water in the pores.

The outcome of this research would be improved overall porosity measurements so that more accurate dispersion coefficient constants determined in this research could be recalculated to consequently calculate more accurate tortuosity factors.

### 6.2.2 Separate Research Recommendations

This subsection is devoted to the area of research that is I discovered to be the weakest area of knowledge – Microdyn colloidal silver inactivation – and I recommend it as the most pressing issue for future research. In addition to colloidal silver inactivation, two more areas of needed future research will be discussed – Electron Microscopic Analysis and Silver Stripping.

To recall, Daniele Lantagne of Alethia Environmental completed a comprehensive study of silver as a microbiological inhibitor (3), but did no study of silver alone. She also documented how Ron Rivera determined the flow rate of the filter by using Microdyn's, the manufacturer of the silver, directions on the bottle. The directions said to put two drops of the 0.32% colloidal silver solution into 2 liters of water and let it stand for 20 minutes (3). Then the water was ready for consumption.

In the United States, water treatment designers and drinking water and wastewater plant operators use a chemical disinfection parameter known as Contact Time (CT). They use the CT parameter for operation and design for optimal inactivation for their individual situations. CT is describes how well a chemical at certain concentration for a determined time will inactivate individual pathogens such as viruses, bacteria, and protozoa. The information is from empirical data.

Currently, Microdyn does not have, or it is not readily available, the information about the CT of their colloidal silver. Research is needed in this area since it will improve the legitimacy of the colloidal silver as a microbiological inhibitor and it will result in improved application of the silver in practice. The primary outcome of this research for Potters For Peace could result in optimal use of the colloidal silver resource i.e. less or more silver with the enhanced performance (better inactivation with less clogging).

I recommend testing different known pathogens that are viruses, bacteria, and protozoa with different concentrations of colloidal silver in the water for varying times. Colloidal silver suspended in water may have different properties from than the silver on the filter. For instance, the colloidal silver in water may have different properties as than the colloidal silver impregnated in the filter. Ideally, the same form of silver used on the filter should be tested along with the

suspended silver to determine CT times. It may be practical to only conduct the suspended form tests. The CT parameter would also be helpful for the silver stripping research recommendation.

As the filter is used, the concentration of silver in the treated water reduces. This is called "silver stripping" meaning that the mass of silver is depleted at an unknown rate over time. I recommend replicating Ms. Lantagne's stripping tests of new filters followed up by a test of the filters after they have been used for certain periods of time. I also recommend measuring the silver concentrations in effluent water of random selections of used filters in Nicaragua to get a gain better understanding of the longevity of the filter as well as a check for current colloidal silver application methods.

The last separate recommendation for research is using the Electron Microscope. To recall in Ms. Lantagne's Report 1, Industrial Analytical Service, Inc. took a portion of the lip of the filter, the least compressed portion of the filter, and analyzed the pore structure. They found that the pore size ranged from 0.6 to 3 microns. I recommend delicately dissecting the filters used in this research after the future research using the filters have been completed. Then the filters could be analyzed for all aspects of the filters including the sides and bottom.

**Section 7.0 Conclusion**

This research is a building block for future research and analysis of the hydraulic properties of the Potters For Peace filter. The initial goals were to find the hydraulic conductivities and tortuosity of the five filters tested. Unfortunately, the hydraulic conductivity results were questionable for many reasons and the tortuosity results varied considerably due to the porosity variability. However, there are some important conclusions found in this study as described below:

- The PFP filter effectively reduced indicator bacteria after 6 months of use in the field from a groundwater source.
- Hydraulics of the filter are complex. This research developed an improved model of the actual conical shape of the filter so it is more applicable to the specifics of the constructed filters.
- Some clogging phenomenon occurred over time in the lab, which is also likely to occur in user homes. This is likely attributed to partial utilization of colloidal silver in the pore structure leaving room for biological growth on the non-lined surface of the pores.
- Further testing of real silver inactivation and hydraulics is needed.

This research may not conclusively describe the hydraulic properties for the PFP ceramic filter, but it does have model improvements and many recommendations for future research. Future work resulting from this research will hopefully lead to accurate and conclusive results about the hydraulic properties of this economically feasible and effective filter.

**Section 8.0 References**

(1) *Project Summary – Tarahumara Filter Project*. Potters For Peace. March 16, 2001.
(2) Lantagne, Daniele. *Investigation of the Potters for Peace Colloidal Silver-Impregnated Ceramic Filter: Intrinsic Effectiveness and Field Performance in Rural Nicaragua*. October 2002.
(3) Lantagne, Daniele. *Investigation of the Potters For Peace Colloidal Silver Impregnated, Ceramic Filter*. Report 1: Intrinsic Effectiveness. December, 2001.
(4) Chemistry: Molecular Nature of Matter and Change. Martin Silberberg. McGraw-Hill Inc. New York, NY.
(5) Maier, Pepper, and Gerba. *Environmental Microbiology*. Academic Press, San Diego. 2000.
(6) *Filtrón Effectiveness: Nitrate Reduction to Nitrite and Turbidity Removal Report*. Emily Heller, David DiGiacomo, Sarah Williams, and Leslie Martien. University of Colorado at Boulder course work. April 2002.
(7) CIRA-UNAN (1999-2001). *Resultados Analíticos de Microbiologia.* Managua, Nicaragua.
(8) Charbeneau, Randall J. *Groundwater Hydraulics and Pollutant Transport*. Prentice Hall. New Jersey. 2000.
(9) Chin, David A. Water-Resources Engineering. Prentice Hall, New Jersey. 2000.
(10) Fetter, C.W. *Contaminant Hydrogeology*. Prentice Hall, New Jersey. 1999.
(11) Eriksen, Sten. *Analysis of Ceramic Filter*. 2001.
(12) Dickenson, Eric. PH.D Candidate University of Colorado at Boulder. Personal Conversation 1/8/03
(13) *Water Quality and Treatment*. American Waterworks Association 4th edition. McGraw Hill, New York .1990.
(14) Merriam-Webster's Collegiate® Dictionary. 10th Edition. 2001.
(15) Xu and Eckstein. *Groundwater*, Vol. 33, No. 6, pp. 905-908. 1995.
(16) Lantagne, Daniele. *Investigation of the Potters For Peace Colloidal Silver Impregnated, Ceramic Filter*. Report 1: Field Investigation. December, 2001.
(17) Rivera, Ron. Email between Potters for Peace and Daniele Lantagne. Fall 2002.

# Appendix A
## Rederivation of the Eriksen Time Equation

$$\tfrac{1}{4}pD^2\,dx = (Q_s + Q_b)\,dt$$

$$Q_s = k\frac{pDx^2}{2a}$$

$$Q_b = k\frac{pD^2x}{4b}$$

$$Q_T = Q_s + Q_b = \tfrac{p}{2}Dk\left(\frac{x^2}{a} + \frac{Dx}{2b}\right) = \tfrac{p}{2}Dk\left(\frac{2bx^2 + Dxa}{2ab}\right)$$

$$Q_T = \frac{pDk}{4ab}\left[x^2(2b) + x(Da)\right]$$

$$\frac{pDD}{4}\,dx = \frac{pDk}{4ab}\left[x^2(2b) + x(Da)\right]dt$$

$$\boxed{\int_x^H \frac{dx}{x^2(2b) + x(Da)} = \int_0^T \frac{k}{Dab}\,dt}$$

$$\int_0^T \frac{k}{Dab}\,dt = T\frac{k}{Dab}$$

The next equation is from a basic integral table.

$$\int \frac{dx}{Ax^2 + Bx + C} = \frac{1}{\sqrt{B^2 - 4AC}}\ln\left|\frac{2Ax + B - \sqrt{B^2 - 4AC}}{2Ax + B + \sqrt{B^2 - 4AC}}\right|$$

The proper substitutions from the boxed equation above were used in the preceding equation for the result below:

$$\int \frac{dx}{x^2(2b) + x(Da) + 0} = \frac{1}{\sqrt{(Da)^2 - 0}}\ln\left|\frac{2(2b)x + Da - \sqrt{(Da)^2 - 0}}{2(2b)x + Da + \sqrt{(Da)^2 - 0}}\right|$$

$$\Rightarrow \frac{1}{Da}\ln\left|\frac{4bx + Da - Da}{4bx + Da + Da}\right|_x^H = \frac{1}{Da}\ln\left|\frac{4bx}{4bx + 2Da}\right|_x^H$$

$$\Rightarrow \frac{1}{Da}\ln\left|\frac{2(2bx)}{2(2bx+Da)}\right|_x^H = \frac{1}{Da}\ln\left|\frac{2bx}{2bx+Da}\right|_x^H = \frac{1}{Da}\left[\ln\left(\frac{2bH}{2bH+Da}\right)-\ln\left(\frac{2bx}{2bx+Da}\right)\right]$$

$$\Rightarrow \frac{1}{Da}\ln\left(\frac{2bH/(2bH+Da)}{2bx/(2bx+Da)}\right)=\frac{1}{Da}\ln\left[\frac{H(2bx+Da)}{x(2bH+Da)}\right]$$

$$\int_x^H \frac{dx}{x^2(2b)+x(Da)} = \frac{1}{Da}\ln\left[\frac{H(2bx+Da)}{x(2bH+Da)}\right] = T\frac{k}{Dab}$$

$$T=\frac{b}{k}\ln\left[\frac{H(2bx+Da)}{x(2bH+Da)}\right]=\frac{b}{k}\ln\left[\frac{H\left(\frac{2bx}{2bH}+\frac{Da}{2bH}\right)}{x\left(\frac{2bH}{2bH}+\frac{Da}{2bH}\right)}\right]=\frac{b}{k}\ln\left[\frac{H\left(\frac{x}{H}+\frac{Da}{2bH}\right)}{x\left(1+\frac{Da}{2bH}\right)}\right]$$

$$\overset{l=\frac{Da}{2bH}}{\Rightarrow}\ \frac{b}{k}\ln\left[\frac{H\left(\frac{x}{H}+l\right)}{x(1+l)}\right]$$

# Appendix B
## Calibration of the Electrical Conductivity Probe

The conductivity probe used was a Hanna Instrument using the 0 to 199.9 µS range. Before each run, the electrical conductivity probe was calibrated using known electrical conductivity solutions. There were seven solutions.

First, using the known manufactured solution of 89.74 µS, the probe was submerged and the conductivity meter's temper gauge was adjusted until it was within 0.4 of 89.74 µS. After the gauge was adjusted, the following solutions were tested with the probe and each measurement was recorded while not adjusting the meter. Solutions 2 through 7 were lab dilutions with Milli-Q® of the manufactured solution.

| Solutions | Electrical Conductivity |
|---|---|
| # | µS |
| 1 | 89.74 |
| 2 | 44.87 |
| 3 | 29.91 |
| 4 | 22.44 |
| 5 | 17.95 |
| 6 | 14.96 |
| 7 | 12.82 |

The values above were the known or true values. After the measurements were taken during this calibration for each solution, the measured values were plotted with the known or true values. The plot was true values versus measured values. From the linear plot, an equation of a line was used to correct the measured values to true values so that each run's measurements were standardized, or calibrated. This calibration made it possible so each run of the filters could be compared to each other.

For example, the first run had a calibration line of $y = 0.9726x + 4.2552$. The measured value (x) was then input into the equation resulting in the true value (y), which was then used in the numerical analysis.

# Appendix C
## Stripping Effect Mass Balance Calculation

Known:
- 2 mL of 3.2% colloidal silver is added to each filter during production
- 3.2% of colloidal silver (Ag) = 32,000 ppm of Ag or mg Ag/L

Assumptions:
- 14 µg Ag/L constant in filter effluent neglecting first few runs
- Filter flow rate = 1.4 L/hr
- Filter used for 16 hours a day
- 14 µg Ag/L is a strong enough concentration for reasonable inactivation of pathogens

Initial silver mass:

$$\frac{32{,}000\ \text{mg Ag}}{\text{L}}\left(\frac{1\ \text{L}}{1000\ \text{mL}}\right)(2\ \text{mL}) = 640\ \text{mg Ag}$$

Silver Stripped over a year (365 days):

$$14\frac{mg}{L}\left(\frac{1\ \text{mg}}{1000\ mg}\right)\left(1.4\frac{L}{hr}\right)\left(16\frac{hr}{day}\right)(365\ \text{days}) = 115\ \text{mg Ag}$$

Amount of excess silver:

$$\frac{640\ \text{mg Ag initially applied}}{115\ \text{mg stripped after one year}} = 5.6 \sim \textbf{6 times more silver}$$

# Appendix D
## Hypothetical Detected Time Method

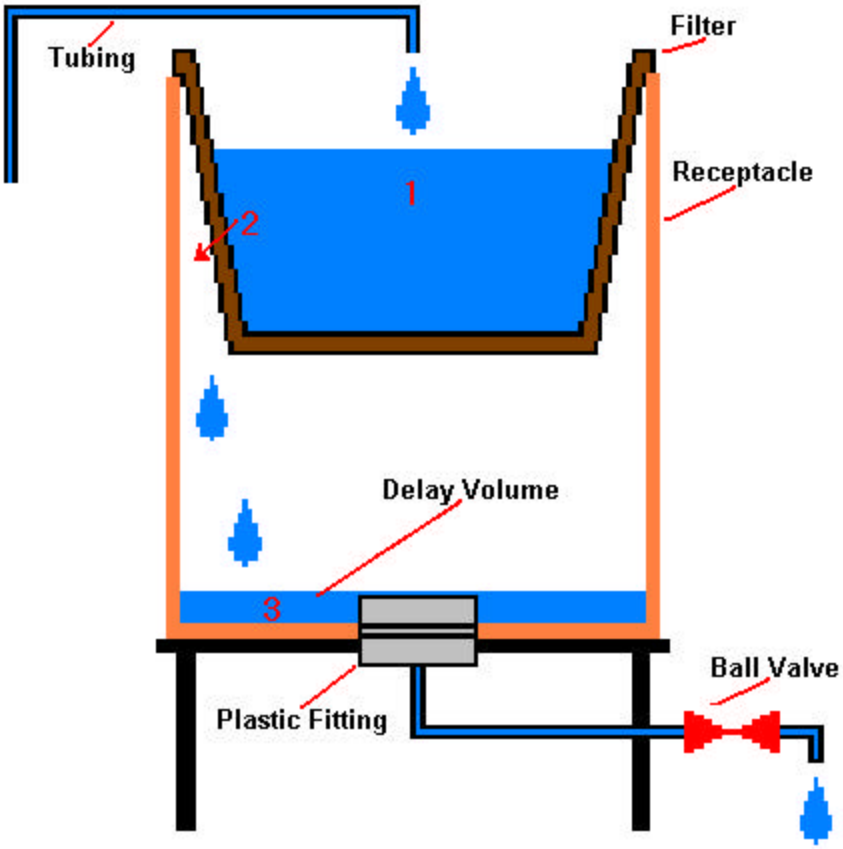


The numbers indicated above represent the sections of the set-up were the water travels. All of the numbers added equal the total amount of time in the filter.

Total time = 1 + 2 +3

The Bromide Tracer was added so it would follow the same path as the water and it would be measured after the ball valve. From the measurements, we would determine the initial and 50% breakthrough times, which were the total time. However, the time in sections 1 and 3 can be estimated and neglected based on an experimental observation and dilution calculation. This results to the total time approximating to section 2, which is the time in the pores.

The smallest change in detectable electrically conductivity was 0.2 µS, the detection threshold. For all of the test runs, the water conductivity entering the filters was about 40 µS. The volume inside the filter (V1) is about 8000 mL for each filter and the largest flow rate during the Bromide Tracer Breakthrough Tests was 45 mL/min (the fastest possible time the tracer could have broke-through and impacted the measurement and time result). Below is the calculation of the dilution time calculation for the time in section 1.

$$\frac{\text{initial } \ mS}{\text{Detection Threshold } (mS)} = \frac{V1}{Qt_1}$$

$$t_1 = \frac{V1 \cdot (\text{Detection Threshold } (mS))}{Q \cdot (\text{initial } \ mS)}$$

$$t_1 = \frac{8000\,\text{mL} \cdot 0.2 mS}{45\,\frac{\text{mL}}{\text{min}} \cdot 40 mS} = 0.89\,\text{min} \ \sim 53\,\text{seconds}$$

The time in section 1 was small so it can be neglected. Furthermore, the time in section 3 can be neglected based on the data taken of the blank during each test run. The shortest time interval of a measurement was ten minutes and each blank experienced an initial tracer breakthrough occurred within ten minutes. Therefore, the time the water was in section 3, the delay volume, can be neglected.

Below is an example of the blank's plot from the fourth run.

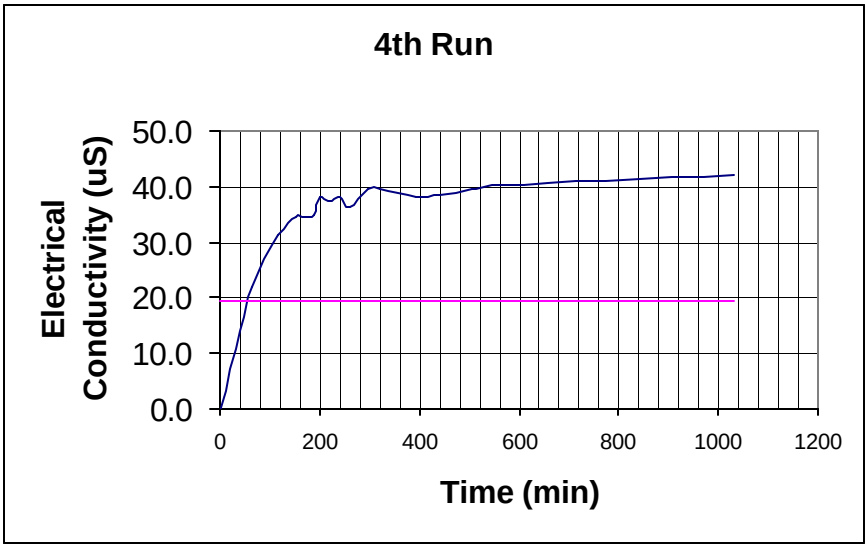

# Appendix E
## Bromide Tracer Breakthrough Test Results for All Filters

Each graph presented will have the title with the appropriate filter number and level of flow (high, medium, and low). The legend for each graph includes the measured values from the experiment, which are the raw data adjusted for calibration and baseline conductivities. The calculated value is the theory or model value obtained using the porosities and dispersion coefficient results.

### Filter 1

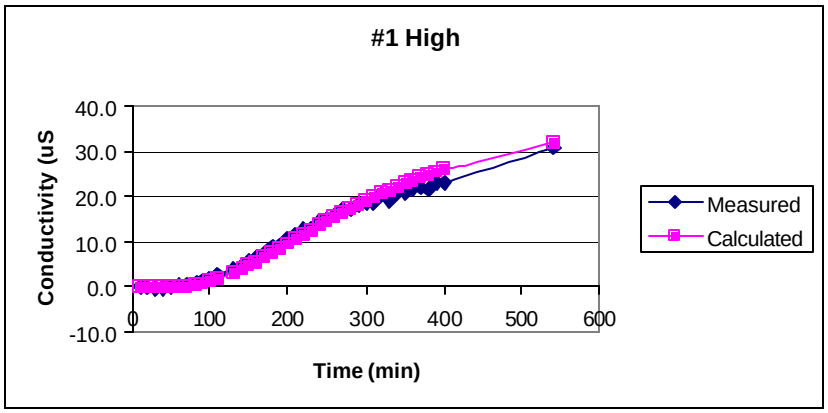


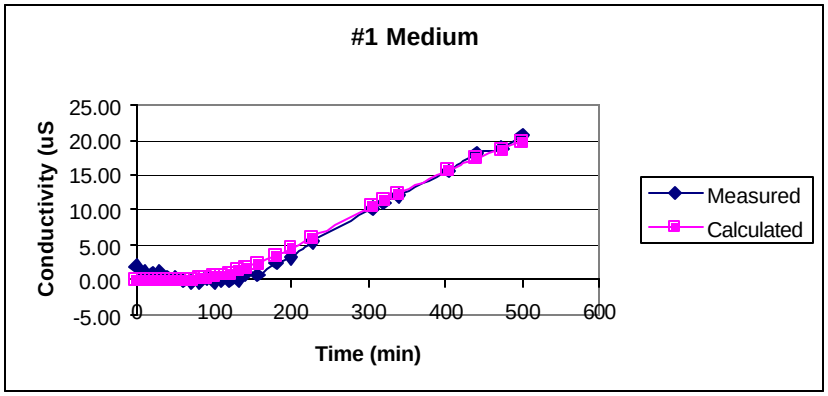


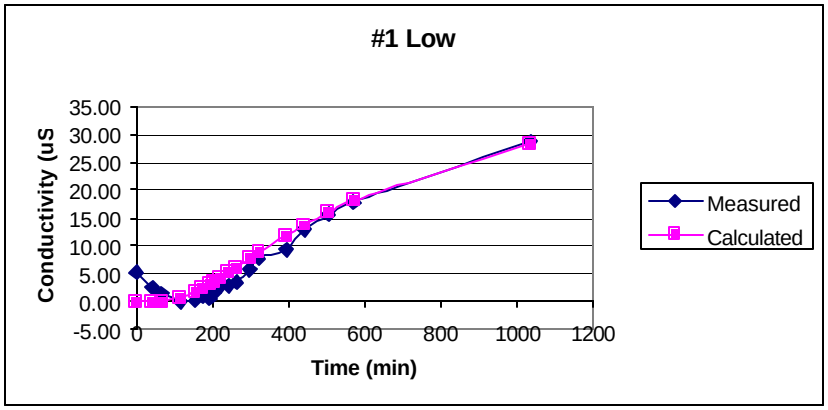

## Filter 2

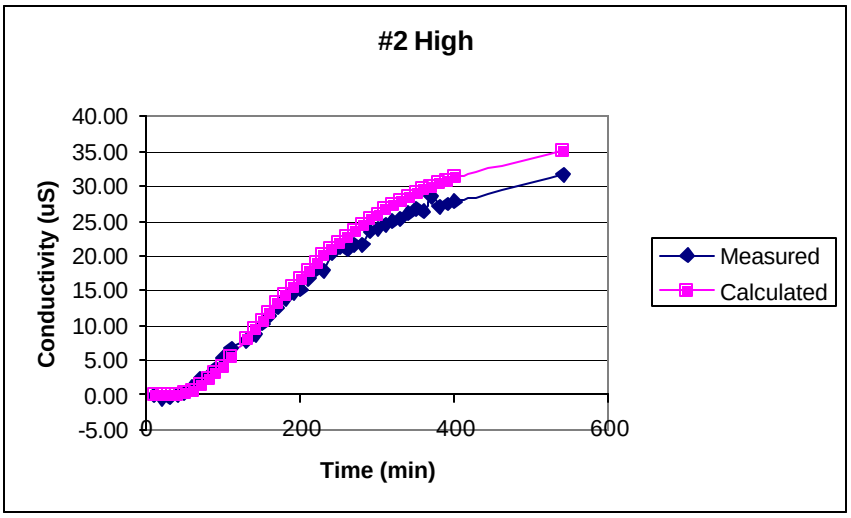
#2 High
Conductivity (uS)
40.00
35.00
30.00
25.00
20.00
15.00
10.00
5.00
0.00
-5.00
0
200
400
600
Time (min)
Measured
Calculated

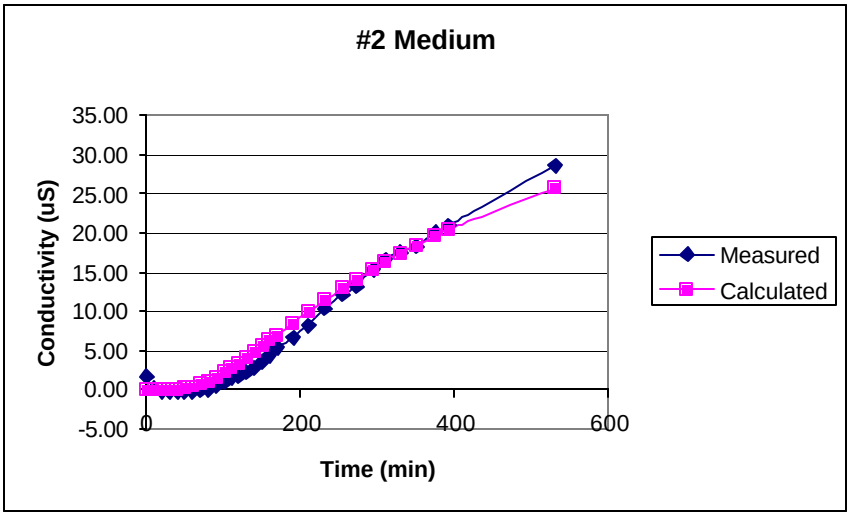
#2 Medium
Conductivity (uS)
35.00
30.00
25.00
20.00
15.00
10.00
5.00
0.00
-5.00
0
200
400
600
Time (min)
Measured
Calculated

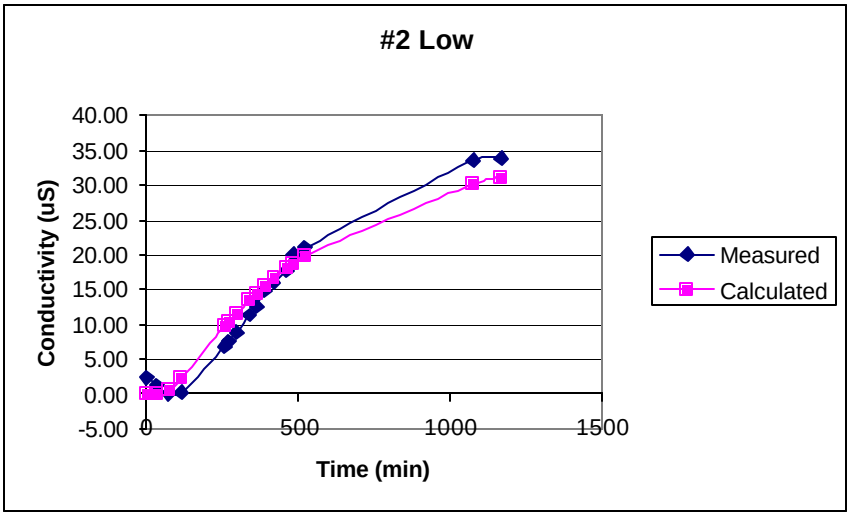
#2 Low
Conductivity (uS)
40.00
35.00
30.00
25.00
20.00
15.00
10.00
5.00
0.00
-5.00
0
500
1000
1500
Time (min)
Measured
Calculated

## Filter 3

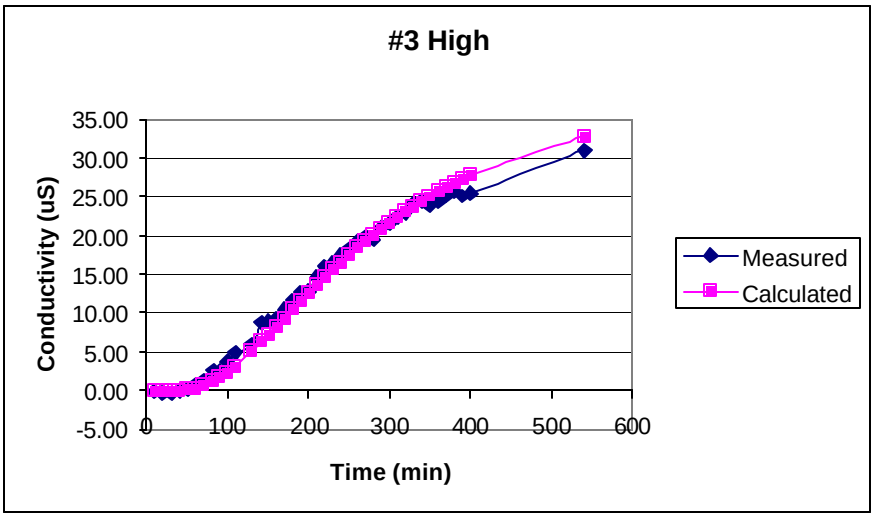
#3 High
Conductivity (uS)
35.00
30.00
25.00
20.00
15.00
10.00
5.00
0.00
-5.00
0
100
200
300
400
500
600
Time (min)
Measured
Calculated

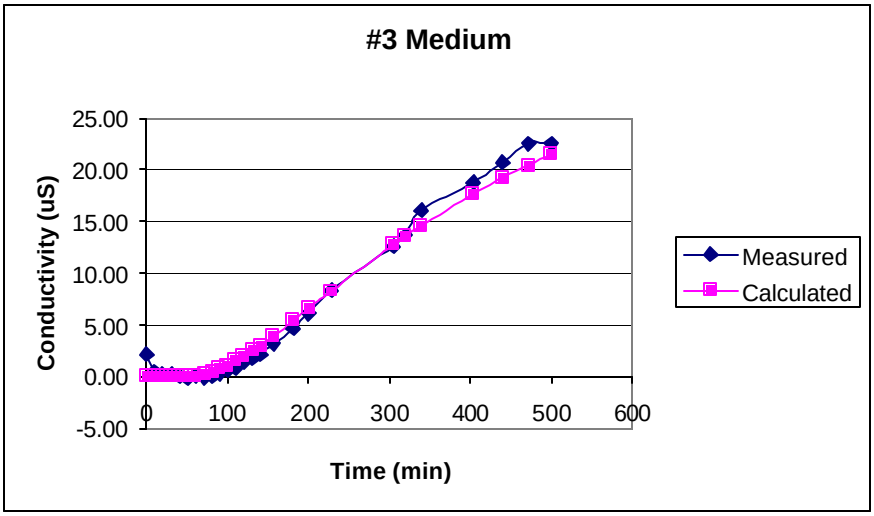
#3 Medium
Conductivity (uS)
25.00
20.00
15.00
10.00
5.00
0.00
-5.00
0
100
200
300
400
500
600
Time (min)
Measured
Calculated

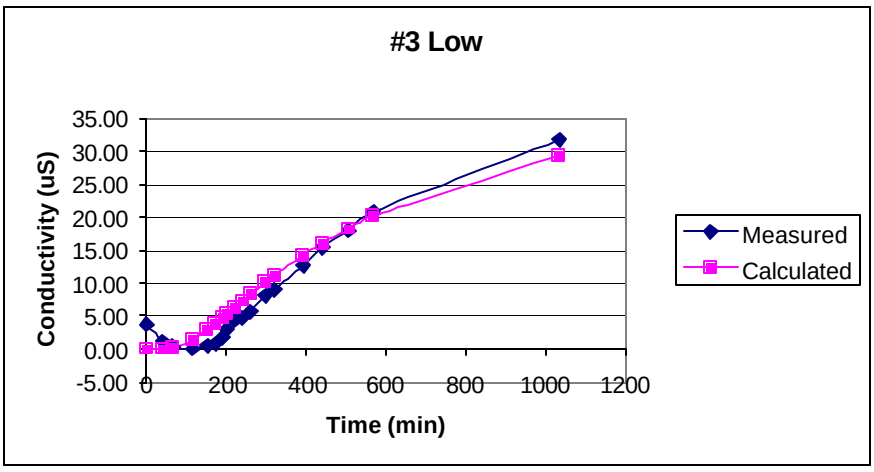
#3 Low
Conductivity (uS)
35.00
30.00
25.00
20.00
15.00
10.00
5.00
0.00
-5.00
0
200
400
600
800
1000
1200
Time (min)
Measured
Calculated

## Filter 4

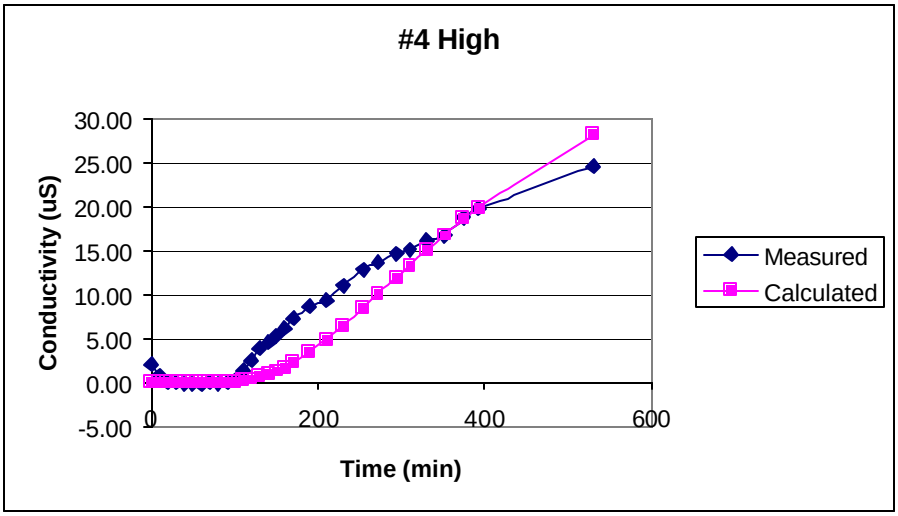
#4 High
Conductivity (uS)
30.00
25.00
20.00
15.00
10.00
5.00
0.00
-5.00
0
200
400
600
Time (min)
Measured
Calculated

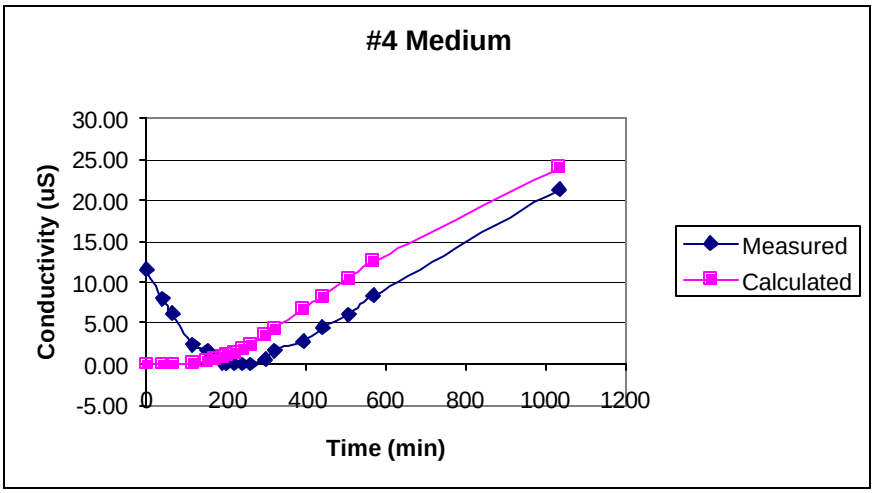
#4 Medium
Conductivity (uS)
30.00
25.00
20.00
15.00
10.00
5.00
0.00
-5.00
0
200
400
600
800
1000
1200
Time (min)
Measured
Calculated

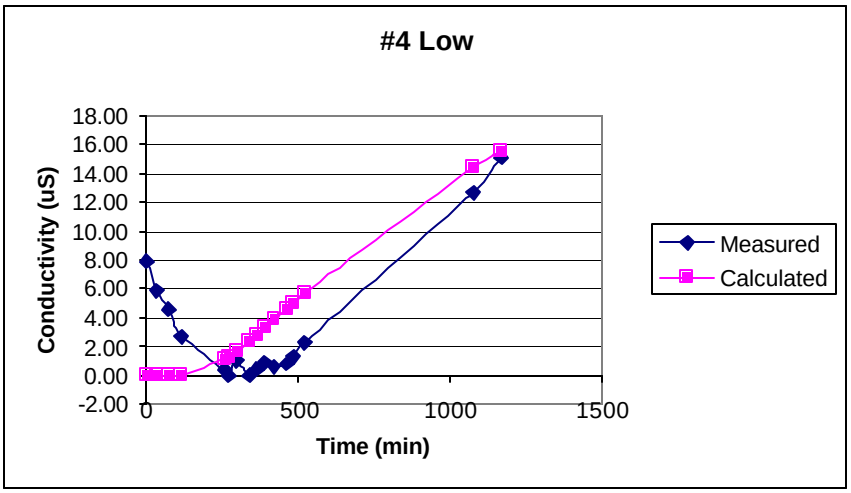
#4 Low
Conductivity (uS)
18.00
16.00
14.00
12.00
10.00
8.00
6.00
4.00
2.00
0.00
-2.00
0
500
1000
1500
Time (min)
Measured
Calculated

## Filter 5

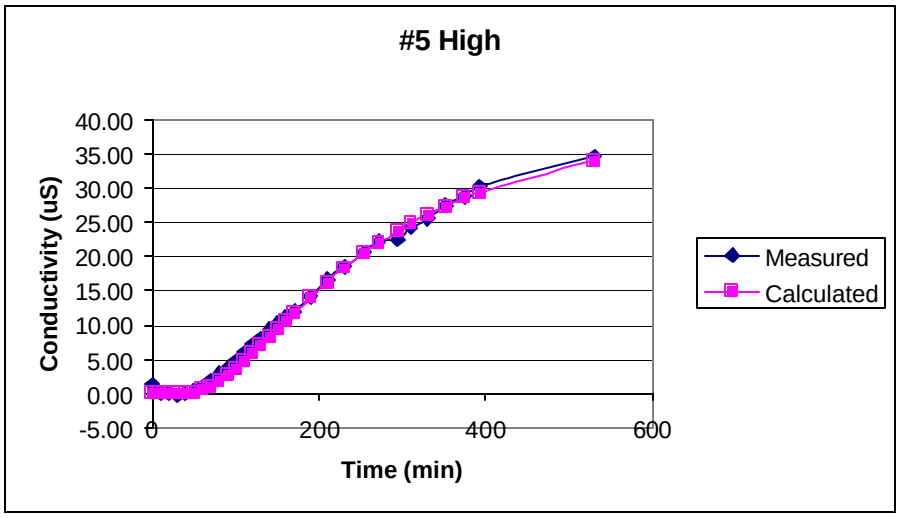
#5 High
Conductivity (uS)
40.00
35.00
30.00
25.00
20.00
15.00
10.00
5.00
0.00
-5.00
0
200
400
600
Time (min)
Measured
Calculated

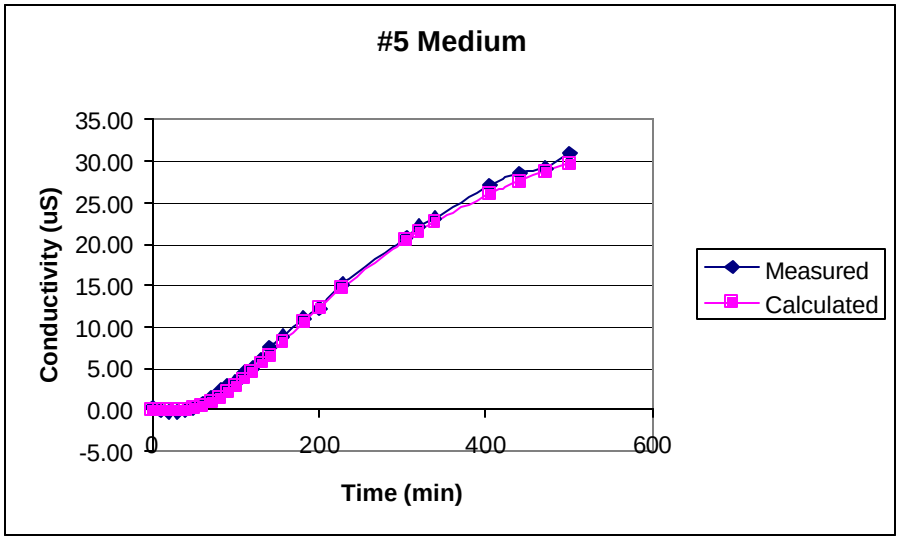
#5 Medium
Conductivity (uS)
35.00
30.00
25.00
20.00
15.00
10.00
5.00
0.00
-5.00
0
200
400
600
Time (min)
Measured
Calculated

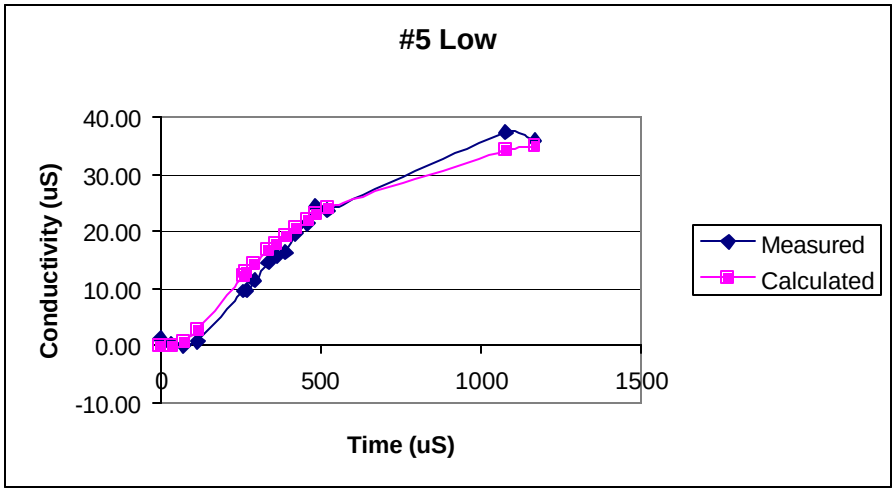
#5 Low
Conductivity (uS)
40.00
30.00
20.00
10.00
0.00
-10.00
0
500
1000
1500
Time (uS)
Measured
Calculated